INFLUENCE OF WETTABILITY ON GAS BUBBLE NUCLEATION

By

RUAA JASIM QADER

Bachelor of Science in Petroleum Engineering

University of Baghdad

Baghdad, Iraq

2006

Submitted to the Faculty of the
Graduate College of the
Oklahoma State University
in partial fulfillment of
the requirements for
the Degree of
MASTER OF SCIENCE
July, 2016

INFLUENCE OF WETTABILITY ON GAS BUBBLE NUCLEATION

Thesis Approved:

Dr. Prem Bikkina

Thesis Adviser

Dr. Sundar Madihally

Dr. Geir Hareland

For My Father’s Soul

ACKNOWLEDGEMENTS

I would like to sincerely thank my advisor Dr. Prem Bikkina, for his constant guidance and unconditional support throughout the period of this research and my study. Without his support, help, and encouragement, this study would not have been possible for me. I would like to express my gratitude for my country and our government (Kurdistan Regional Government) for their support without them I could not fulfill this achievement.

I would like to extend my thanks to the other members of my committee, Dr. Sundar Madihally and Dr. Geir Hareland for their valuable time to review my thesis and their valuable inputs. I would also like to thank the School of Chemical Engineering at Oklahoma State University for their valuable assistance during the course of my graduate studies. I would also like to thank my colleague Subarna Kole for her support and help. I would like to thank my beloved husband (Dr. Ali Abdullah) who supported me and encouraged me through my journey without his support I could not achieve my goal. Also, I would like to thank my mother for her deeply support and encouragement. Moreover, I would to thank my family in-law for their support and encouragement.

Name: RUAA JASIM QADER

Date of Degree: JULY, 2016

Title of Study: INFLUENCE OF WETTABILITY ON GAS BUBBLE NUCLEATION
Major Field: CHEMICAL ENGINEERING

Abstract: Gas bubble nucleation and liberation from supersaturated liquid solutions takes place in a wide range of natural and industrial processes, such as volcanic eruption, cloud formation, production of carbonated drinks, manufacturing of polymers, electrochemical processes, and petroleum production and refinery systems. Bubble nucleation from a liquid system is the first step of gas liberation process. Usually, the bubble nucleation begins on vessel and/or solid particles (if any) surfaces.

The aim of this research was to experimentally study the effect of wettability on gas bubble nucleation. An experimental facility that can provide high levels of supersaturation and control pressure during step-down process was designed and built. The design of the research depends on providing a continuous source of CO_2 (gas phase), which can be pressurized and transferred into a pressure cell that contains a glass vial filled with water (liquid phase) to a specified height. Hydrophilic and hydrophobic vials and glass beads were used for the bubble nucleation experiments. Chlorinated polydimethylsiloxane (CM) and chlorinated fluoroalkylmethylsiloxane (CF) coatings were implemented on the glass vials and beads to obtain hydrophobic surfaces. A pulseless pressure of CO_2 was supplied by utilizing a microfluidic P-Pump that could provide a pressure range of 0-10 bar to the vial in the pressure cell. Semi-infinite diffusion equation for planar geometry was used to estimate the time required for CO_2 to reach the equilibrium concentration. 6000 mbar pressure for 24 hour saturation time was applied to the pressure cell to saturate CO_2 in 5 mm height of water in a 10 mm ID glass vial. 1000, 500 and 100 mbar step-down pressures were used to initiate pressure-driven bubble nucleation process. A digital microscope was used to record high quality pictures and videos of the bubble nucleation process. All the experiments were performed at room temperature 25 °C (77 °F). Contact angle, atomic force microscopy (AFM) and X-ray photoelectron spectroscopy (XPS) measurements were conducted for the treated and untreated glass substrates for wettability, surface roughness, and surface chemistry, respectively.

Hydrophilic vials did not cause bubble nucleation even when the pressure was reduced to atmospheric pressure. However, both the CM and CF coated hydrophobic vials resulted bubble nucleation during the pressure releasing process. The results of using hydrophilic and hydrophobic glass beads inside hydrophilic vial confirmed the effect of wettability on gas bubble nucleation. So, it can be concluded that wettability alteration of the solid surfaces using coating techniques can enhance the rate of pressure-driven bubble nucleation.

TABLE OF CONTENTS

LIST OF TABLES

LIST OF FIGURES

CHAPTER I

INTRODUCTION

Nucleation begins at a small region, which is called nucleus, and it is associated with any appearance of new phase embryos. It generally occurs due to a chemical or a physical change in the material system (Maris, 2006). Nucleation and bubble growth are very important since these phenomena are widely encountered in various industrial processes such as polymer devolatilisation, production of carbonated drinks, electrochemical cells, and heavy oil production (Yang et al., 1997; Wienecke et al., 2005; Liger-Belair et al., 2006; Hua et al., 2002; Jones et al., 2009; Lillico et al., 2001). There are many examples in nature that exhibit bubble nucleation, for example, rainfall, water freezing, cloud formation, crystallization, and lava flow from volcanoes (Pruppacher and Klett, 2010; Sear, 2007; Cashman et al., 1994).

The research history on bubble nucleation began in the 16th century and from then investigations have been carried out to understand the factors that may influence bubble nucleation, growth and liberation. Anisimov et al. (2009) summarized the experimental methods and results on vapor-liquid bubble nucleation from the published literature and concluded that there were substantial inconsistencies possibly originated from using different types of experimental approaches that could have introduced an uncontrolled parameter. Frenkel (1955) and Skripov (1974) suggested that it is very important to utilize pure liquids and clean environment to systematically study the parameters that affects bubble nucleation in vapor-liquid systems.

In oil and gas industry, gas bubble nucleation kinetics can play a big role at different stages of production and equipment design. In oil reservoirs, gas bubble nucleation occurs when the pressure reaches at or below bubble point. As the pressure continues to decline, more and more bubbles will nucleate and coalesce to form larger bubbles and contribute to

production as solution-gas drive (Chen, 2006; Lillico et al. 2001). In gas-oil separation systems, bubble nucleation kinetics influence separator design (Kalikmanov et al., 2007). Pre-existing gas cavities is one of the significant factors that can assist gas bubble nucleation in a single phase liquid. Higher supersaturation levels would be required to nucleate bubbles if there are no gas cavities (Jones et al., 1999; lubetkin, 1995; Kumar and Weller, 1994).

In high supersaturation systems, as the amount of the solute increases, the corresponding amount of solvent decreases. For example, in the case of CO_2 dissolved in water at a super saturation ratio of 5, there are 414 water molecules for each molecule of CO_2. At a higher super saturation ratio of 2000, there would be 1 molecule of water for each molecule of CO_2 (Cyr, 2001).

Gas solubility relies on pressure and temperature. In general, as the pressure increases, gas solubility in a liquid increases, as it is stated in Henry's law. A common example that can illustrate Henry's law is the production of carbonated drinks. To dissolve CO_2 and reach high levels of saturation in a liquid, a pressure higher than atmospheric pressure is required. CO_2 is dissolved at a pressure of 3039.75 mbar in water for Minto's drinks (Coffey, 2008). Bubble nucleation can happen before or after opening the soda bottle. Bubble nucleation in the bottle governs by Henry's law at a constant temperature. Henry's law is illustrated in equation 1.1

$$\boldsymbol{P = kC} \qquad \textbf{Equation 1.1}$$

where,

P = Partial pressure of gas (CO_2 in the above example)

k = Henry's law constant parameter

C = Molar concentration of dissolved solute (CO_2).

In the process of opening the soda bottle, the equilibrium inside the bottle will be broken. The partial pressure will be dropped which causes the CO_2 equilibrium concentration to drop and then the gas bubbles nucleate. The dissolved gas requires nucleation sites to nucleate and form bubbles. Temperature is another important factor for

bubble nucleation. Rise in temperature can increase the amount of the formed bubbles and causes reduction in the Henry's law constant (K) (Hikita and Konishi, 1984).

CHAPTER II

LITERATURE REVIEW

2.1 Classical Nucleation Theory

Classical bubble nucleation Investigation was begun by Gibbs when he conducted his experiments using critical radius size for studying bubble nucleation (Cyr, 2001). Classical nucleation theory assumes that forming bubbles in supersaturated liquid solution would be initiated at a bubble size of zero (Cyr, 2001). Gibbs assumed that after nucleation and bubble formation step, the process of bubble growth will continue if it is bigger than the critical size and bubbles will shrink process if it is smaller than the critical size (Cyr, 2001; Wilt, 1986; Lubetkin and Blackwell, 1988; Leung, 2009; Tucker and Ward, 1975).

Based on the substance, purity, and the environment, classical nucleation is categorized into homogenous and heterogeneous bubble nucleation. Based on thermodynamic analysis, bubble nucleation occurs when there is enough energy that would cause gas bubbles to nucleate and to form (Blander and Katz, 1975; Jones et al., 1999). Bubble nucleation in heat-flux boiling system can be affected by the liquid, interfacial, and solid substrate properties (Blander and Katz, 1975). In nucleation processes, there exists an energy barrier that should be overcome to cause bubble nucleation. The energy barrier can be directly affected by the interface existence and its physicochemical properties. If no interface is involved in the nucleation process, it is called as homogenous bubble nucleation (Lubetkin, 1995). Blander and Katz (1975) stated that homogenous bubble nucleation occurs inside the bulk liquid, while heterogeneous bubble nucleation occurs at solid-liquid interface. In heat-flux systems, homogenous bubble nucleation requires a higher temperature to occur than heterogeneous bubble nucleation (Blander and Katz, 1975)

Harvey et al. (1944a & 1944b) through conducting his research on animal's cells, recognized that the presence of pre-existing gas bubbles may play a significant role in bubble nucleation from supersaturated solutions. He mentioned that any tiny gas nuclei on the cell surfaces could initiate bubbles. Later, this phenomenon was named after him. Wilt (1986) stated that a large amount of gas bubbles canbe formed on the vessel's wall using low supersaturated levels of 3 to 5 because of the presence of pre-existing gas liquid interface. Harvey et al. (1947) conducted a research to determine the speed of the rods, with and without pre-existing gas nuclei, being immersed in a supersaturated liquid that causes bubble nucleation. A speed of 3 m/s was required to form bubbles on the rod with gas nuclei, whereas a 37 m/s velocity was required to form bubbles on the rod without pre-existing gas nuclei.

Franka et al. (2007) investigated bubble nucleation and growth using carbon dioxide and different Newtonian and non-Newtonian liquids. Varied pressures were applied to saturate CO_2 in the liquids. They observed a rapid bubble growth followed by a linear increase in the bubble size with time till a critical size is reached and then the bubble detaches and grows exponentially while it is rising from the immobile nucleation site.

Jones et al. (1999) claimed that both homogenous and heterogeneous bubble nucleation require saturation levels more than 100. Wilt (1986) did a study on bubble nucleation by saturating CO_2 in water. He mentioned that bubble nucleation will occur for both classical types of nucleation at superstations ranged from 1100 to 1700. Whereas other studies reported that heterogeneous bubble nucleation occurs at very low levels of supersaturation of around 2 to 8 for CO_2 in water system (Lubetkin and Blackwell, 1988).

2.2 Homogenous Bubble Nucleation

Homogenous bubble nucleation is defined as the nucleation that takes place in the bulk liquid itself (Fsadni et al., 2012). A pure liquid is required to have this type of nucleation while heterogeneous bubble nucleation does not need a pure liquid to encourage bubble nucleation (Delale et al., 2003). Wilt (1986) mentioned by studying CO_2 saturated

in water that high levels of superstation is required to obtain homogenous bubble nucleation (Wilt, 1986). It also can occur when there are pressure differences between the dissolved gas surface and the ambient pressure (Harvey et al., 1975; Wilt, 1986). The eruption of a volcano and explosive boiling are natural processes that are related to homogenous bubble nucleation (Delale et al., 2003). In heat-flux systems, super-cooling or super-heating system is required to obtain homogenous bubble nucleation (Leung, 2009). Polymer production is also one of the homogenous bubble nucleation examples in industrial processes (Leung, 2009).

2.3 Heterogeneous Bubble Nucleation

Heterogeneous bubble nucleation happens at solid-liquid interfaces (Blander and Katz, 1975). In a boiling system, this type of nucleation is required a lower temperature than homogenous nucleation to take place (Blander and Katz, 1975). Hey et al. (1994) mentioned that pre-existing gas is a preferred system for heterogeneous nucleation, especially with rough solid surfaces that contain cracks.

2.4 Wettability

Wettability is a physical parameter that plays a significant role in a variety of natural and industrial processes. It can be defined “as the tendency of one fluid of a fluid pair to coat the surface of a solid spontaneously”, according to Jerauld and Rathmell (1997). In other words, it is a fluid’s tendency to spread on a solid surface in the presence of a second fluid depending on the interaction between the three phases.

Anderson (1986) mentioned in his report that contact angle measurement can be used to determine the fluid wetting degree on a solid surface. Some of the applications that relate to the wettability phenomenon are: oil recovery, boiling heat systems, coatings and sprays, glass manufacturing, soil science, soaps and surfactants (Prabhu et al., 2009; Zhao et al., 2010; Wang et al., 2010; Sakai et al., 2009; Son et al., 2008; Perelaer et al., 2009; Yang and Jiang, 2010; Bhushan et al., 2009; De Gennes, 2004). Wettability also plays a critical role in selecting carbon dioxide sequestration sites (Bikkina, 2011).

A surface is called hydrophilic if water spreads on it and hydrophobic if water repels. Hydrophilicity and hydrophobicity degrees can be quantified utilizing contact angle

measurement as mentioned before. The surface will be called super-hydrophobic when its air-water contact angle value exceeds 150^{o}. In this case, there is almost no contact between the water drop and the surface. Having 0^{o} contact angle indicates complete wetting and the liquid droplet completely spreads on the solid surface (Lafuma and Quere, 2003; Jo et al., 2011).

DeGnnes, (2004) suggested the following equation for determining wettability.

$$\boldsymbol{S = \sigma_{SV} - (\sigma_{SL} - \sigma_{LV})} \qquad \textbf{Equation 2.1}$$

where,

S is spreading parameter that depends on the surface tension of solid, liquid, and gas.

σ_{SV} = surface tension solid/vapor interface

σ_{SL} = Surface tension of solid/liquid interface

σ_{lV} = surface tension liquid/vapor interface

When S is greater than 0, it means that there is a complete wetting of substrate. Metal surfaces are considered as the best examples to show this type of behavior and its surface tension (surface energy) values are around ≈500-5000 mN m^{-1}. When S value is smaller than 0, Partial wetting will occur with the solid substrate.

A solid surface is called hydrophobic when the contact angle is higher than 90^{o} (non-wetting surface). Hydrophobic behavior can occur when the values of σ_{SV} are between 10 to 50 mN m^{-1}, for example when using a plastic substrate.

Jo et al. (2011) investigated the influence of wettability on heat-flux bubble nucleation. The results showed that both 54^{o} contact angle hydrophilic wetting surface (SiO_2) and 123^{o} contact angle hydrophobic surface (Teflon) caused heterogeneous bubble nucleation even without the presence of micron sized surface roughness. The authors mentioned that utilizing hydrophobic surfaces would be more efficient than using hydrophilic surfaces since nucleating bubbles using hydrophilic surfaces needs higher heat flux regime.

Attinger (2014) mentioned in his study that wettability can be modeled into engineering texture and chemistry. Different materials can be utilized to induce new surface textures, such as using coating processes on smooth solid hydrophilic substrates. Adding surfactants to the liquid phase and lower its surface tension can be useful for changing wetting specifications (Wen and Wang, 2002; Bico et al., 2002; Abe, 2004; Phan et al., 2009). Yuan et al. (2016) stated that wettability and topography of the solid surfaces may have effect on bubble nucleation in heat-flux systems

It is important to study wettability effect on pressure-driven bubble nucleation since it has been reported that it has an influence on nucleating bubbles in heat-flux (temperature-driven) bubble nucleation (Phan et al., 2009). Wettability treatment on hydrophilic surfaces can provide hydrophobic surfaces that may be used for enhancing bubble nucleation (de Gennes et al. 2004). This technique may be used in pressure-driven bubble nucleation since there are many examples that refer to the success of using wettability alteration. For example, wettability alteration technique showed its ability to produce improved oil recovery (Abe, 2004). It has also been used to alter the wettability of porous media from preferential liquid wetting to gas wetting. This alteration may increase the deliverability of gas-well in the gas-condensate reservoirs (Kewen and Abbas, 2000). In oil-wet carbonate reservoirs, oil recovery can be increased using wettability alteration methods (Karimi et al., 2012).

2.5 Roughness

Roughness is a surface texture component. The effect of roughness is important in various processes such as the fluid pressure drop in flow through a mini channel and (Kandlikar et al., 2005). Ryan and Hemmingsen (1993&1998) conducted experiments to investigate the influence of roughness and wettability on pressure-driven bubble nucleation. The solid phases used in these experiments were smooth and rough hydrophilic and hydrophobic submicron sized polystyrene and silica particles. The liquid phase was water and the gas phase was N_2. The experiments were conducted at room temperature. Supersaturation gas pressures were ranged from 5 to 125 atm. Even high supersaturation levels did not encourage bubbles to nucleate on both smooth hydrophobic and hydrophilic surfaces since water molecules have high surface tension. Bubble nucleation depends on

rapturing the surface tension force of water molecules. So, smooth surfaces do not have this ability to minimize or rapture surface tension force of water (Ryan and Hemmingsen, 1993). Whereas rough hydrophilic and hydrophobic surfaces could promote bubble nucleation even with solutions of much lower supersaturation levels.

A series of experiments were conducted by Kurihara and Myers (1960) to investigate surface roughness effect on boiling coefficients. In this experiment, water, n-hexane, and acetone were boiled on a flat surface. The results showed that increase in surface roughness would lead to increase in boiling coefficients. Attinger et al. (2014) focused on finding the influence of roughness on wettability for bubble nucleation in heat-flux boiling process. It was reported that change in surface roughness can alter contact angle values.

Johnson and Dettre (1964) conducted a study to find the influence of roughness on advancing and receding contact angles. The authors used a waxed surface to conduct this research since the wax material has constant chemical properties. The outcomes of this type of experiment indicated that increasing in roughness factor may result a higher value of contact angle in the case of hydrophobic surfaces.

Wenzel (1936) conducted a study on finding a connection between surface roughness and wettability. He found that hydrophobicity can be enhanced by increasing surface roughness. Wenzel theory is shown in the following equation.

$$\boldsymbol{Cos\theta_m = r\, Cos\theta} \qquad \textbf{Equation 2.2}$$

where,

θ_m = the measured contact angle

θ = the Young's model angle

r = a surface roughness ratio that can be calculated by measuring the ratio of true area to the apparent area of the surface.

2.6 Surface Tension and Interfacial Tension

Surface tension is considered as an important parameter that can provide accurate information regarding surfaces and the intermolecular interactions (Begheri et al., 2016).

Barati-Harooni et al. (2016) defined interfacial tension (IFT) as “a term refers normally to the boundary between two or more co-existence immiscible fluids”. Molecular interactions at the interface are different from the molecules in the bulk liquid.

It is important to highlight that surface tension forces play an important role in bubble nucleation (Coffey, 2008). High surface tension hinders bubble nucleation since the cohesive forces of the liquid solution is higher than adhesive forces. Solute gas molecules will gather near the nucleation site until it reaches the point of rupturing the high surface tension of the solvent to nucleate and form bubbles.

Dean (1944) observed that large number of bubbles form during the turbulent flow of supersaturated liquid solutions or when the solutions are vibrated. Franka et al. (2007) in his study of CO_2 bubble nucleation included a vibrating system in his experimental design to accelerate the process of supersaturating CO_2 in the solution. Shaking a soda bottle before opening shows the effect of using this mechanism on bubble nucleation rate. It is known that soda is bottled under high pressure of carbon dioxide, which surpasses the carbon dioxide solubility in the liquid solution. During the shaking, some of the CO_2 gas molecules will be mixed with liquid until it will be supersaturated in the solution. At opening the lid, many of CO_2 gas bubbles will be liberated, because bubbles could rupture liquid surface tension(Venter et al., 2001).

Pressure can be an important factor that can affect interfacial tension properties. Interfacial tension is used to calculate the enhanced oil and gas recovery efficiency and it is also used to determine the CO_2 storage capacity of geological formations (Espinoza and Santamarina, 2010). The authors measured high pressure (up to 20 MPa) contact angle and interfacial tension data for CO_2-water-mineral systems. The results showed that increase in pressure reduces interfacial tension between CO_2 and water. Temperature can affect surface/interfacial tension. A recent study by Bagheri and Bakhshaei (2016) showed that surface tension decreases by increase in temperature of different mixtures of dimethyl sulfoxide and methanol, ethanol, or isopropanol. Bikkina et al. (2011) reported that increase in temperature increases the IFT between CO_2 and water when the CO_2 is a gaseous phase whereas the IFT is mostly insensitive to temperature when the CO_2 is a liquid or supercritical phase.

Water has a high surface tension of about $72x10^{-3}$ N/m (Vargaftik et al., 1983). This strong force comes from the high bonding of hydrogen molecules that makes a barrier to any dissolved gas such as, CO_2, to nucleate from water and leave the water surface. In diet coke drinks manufacturing, gelatin and Arabic gum are used to lower water surface tension and allow CO_2 gas bubbles leave water surface (Coffey, 2008). Studying interfacial tension can be useful for minimizing the time required to liberate gases from liquids.

2.7 XPS Measurement

X-ray photoelectron spectroscopy (XPS) is one of the important innovations that have the ability to provide precise surface chemistry information. XPS is a technique that can measure the compositions of the elements with both chemical and electrical states of the elements. This device works by irradiating X-rays beam on the material surface. During the irradiation, the kinetic energy and electron numbers of the element will be measured. XPS device can be operated at ambient pressure and also under high vacuum. In this research, XPS will be utilized to compare the surface chemistry of glass substrates before and after hydrophobic coatings.

2.8 AFM measurement

Experiments showed that roughness can alter wetting degrees for high or low energy substrates since it changes surface properties (Miller et al., 1996). Atomic force microscopy (AFM) can be used to measure surface roughness of solid substrates. AFM can provide information about surface forces including wettability, surfactant self-assembly, lubrication, and colloid stability (Ducker and Senden, 1992). A sharp tip and the tip support, which is called a cantilever, control the process of obtaining a topographic image. Both the tip and the cantilever scan the area that intended to be measured. The reflection of the tip and the cantilever will be transformed to a high-resolution image. In this study AFM was used to obtain 2-dimentional (2D) and 3-dimensional (3D) surface topographic images of the coated (hydrophobic) and uncoated (hydrophilic) surfaces.

CHAPTER III

EXPERIMENTAL SECTION

In this research, new facility was designed to form CO_2 gas bubble nucleation from a supersaturated solution. In the designed facility, CO_2 gas was generated by a gas cylinder, CO_2 saturation and stepdown pressure were performed by P-Pump microfluidic device. Hydrophilic and hydrophobic (CM and CF) surfaces were utilized, and measured to explore wetting degree, surface roughness, and chemistry surface. Thus, the wettability effects on pressure-driven bubble nucleation could be investigated. The following sections describe the process in detail.

3.1 Experimental Facility

The aim of this research was saturating CO_2 in water at a specific pressure and study pressure-driven bubble nucleation on the surfaces of various wetting degrees. For this purpose, a microfluidics facility was built and used. The facility consists the following components:

1. A CO_2 supply
2. A three-way valve
3. A pressure relief valve (PRV)
4. A microfluidic pump
5. A pressure cell (flow site)
6. A small glass vial
7. A valve to flush air from the pressure cell
8. A digital microscope

The functions of the above components are explained in the following paragraphs. Figure 3.1 shows the schematic of the experimental setup used for the bubble nucleation experiments.

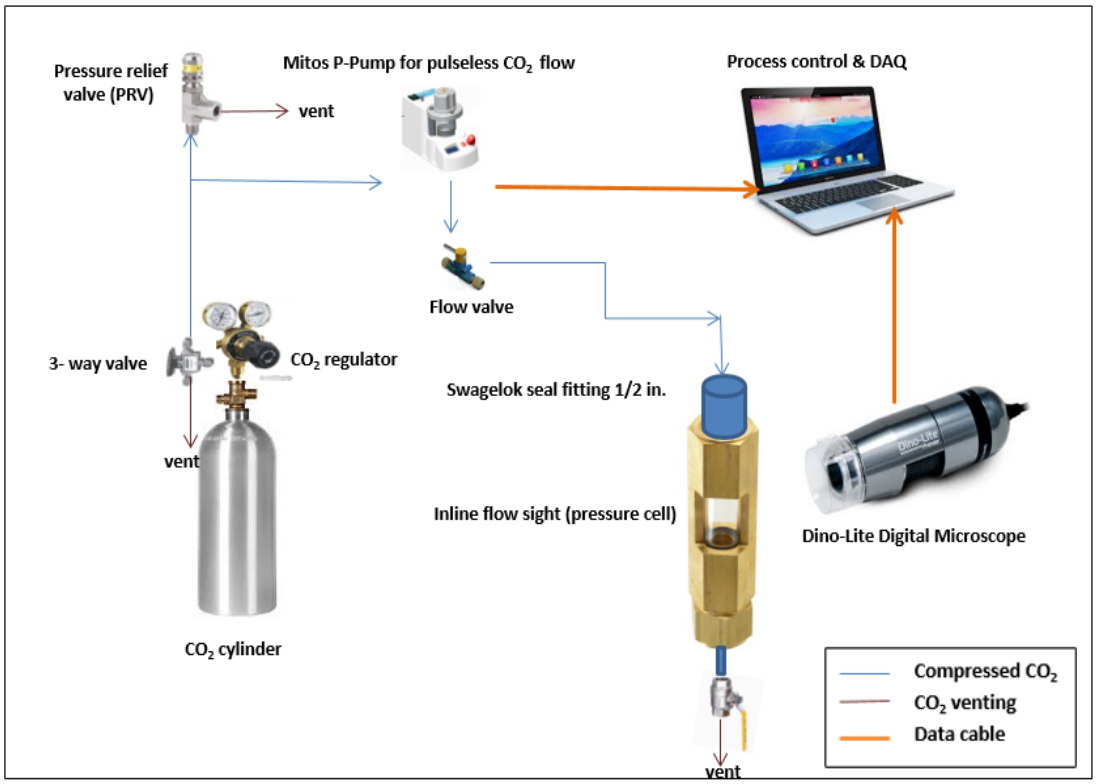

Figure 3.1: Schematic of the experimental setup used for bubble nucleation experiments

The gas cylinder was used to provide a continuous flow of high purity CO_2 (99.99%) to avoid any possible contamination from the gas phase for bubble nucleation experiments. The low pressure side of the cylinder regulator was connected with a three-way valve. One of the outlets of the three-way valve was connected to snorkel to vent CO_2, for safety purposes, after finishing the experiment. The other outlet was connected to the P-Pump through the PRV that was set at 125 psi (8618.45 mbar) to prevent damaging the high sensitivity P-Pump which should not be exposed to pressures above 10000 mbar. The releasing side of the PRV is connected to the vent.

The P-Pump is the most critical part of the microfluidic facility. It is capable of providing a pulseless control of fluid flow (30 – 1000 µL/min) and pressure (0 - 10000 mbar range) which are necessary for the bubble nucleation experiments. This device is provided with software called Flow Control Center. The software allows choosing to control pressure or flow rate according to the nature of the experiments to be conducted.

In addition, it contains the option to observe and save the pressure and flow rate data. Figure 3.2 shows the Mitos P-Pump

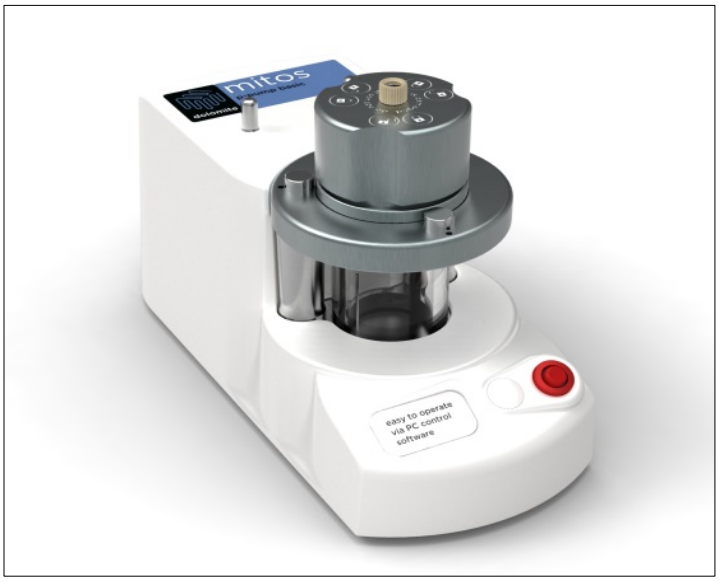

Figure 3.2: Mitos P-Pump

The microfluidic P-Pump was used to transfer CO_2 to the pressure cell. P-Pump was used to provide CO_2 that would saturate in water and also to control pressure step-down process. It offers a safe environment since small amounts of CO_2 was used. The data acquisition will be saved in the computer in the form of an Excel sheet. Figure 3.3 and 3.4 show Flow Control Center, and a sample from Excel sheet data respectively.

The pressure cell is made of brass, glass, and plastic/rubber seal materials. Using it directly would affect bubble nucleation process as there are multiple materials and surfaces, so it was decided to insert a glass vial that contains water inside the cell to conduct the test. Including the transparent glass in the flow sight made it easy to visualize the nucleation process and capture the pictures for documenting purposes.

While conducting bubble nucleation experiments, the cell was sealed. One side of the pressure cell was connected to the P-Pump using a 1/16” OD and 250 µm ID tube to transfer CO_2 to the pressure cell. The other side of the cell was connected to a valve that was used to flush out any trapped air inside the cell by flowing CO_2 at 200 mbar for 30

minutes at the beginning of the saturation time. The dimensions of the cylindrical glass vial that was used for bubble nucleation experiments were 12 mm diameter x 25 mm height.

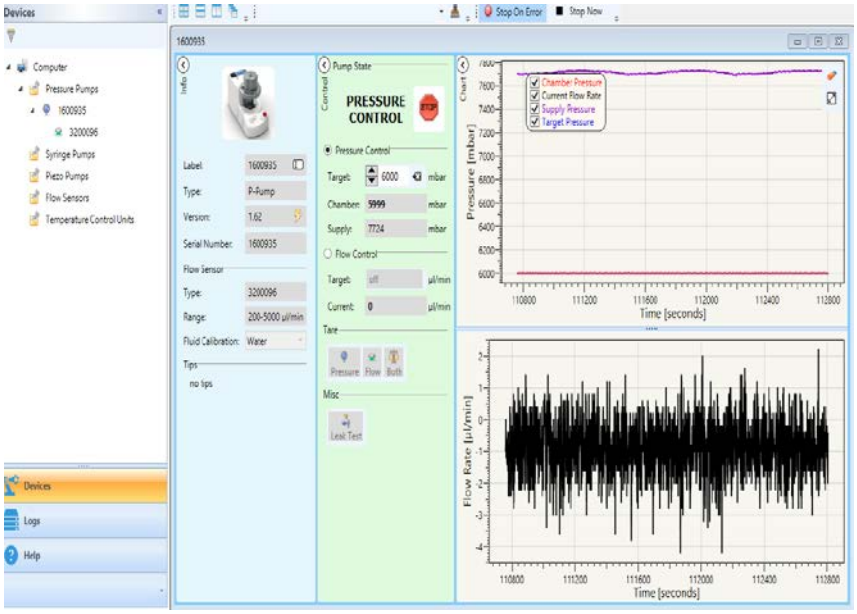

Figure 3.3: Flow Control Center

I11

	A	B	C	D
1	Date/Time [Locale = English (United States), M/d/yyyy h:mm:ss tt]	Chamber Pressure [mbar]	Target Pressure [mbar]	Supply Pressure [mbar]
2	4/27/2016 11:49	6005	6000	7803
3	4/27/2016 11:49	6004	6000	7805
4	4/27/2016 11:49	6002	6000	7806
5	4/27/2016 11:49	6002	6000	7807
6	4/27/2016 11:49	6002	6000	7808
7	4/27/2016 11:49	6001	6000	7809
8	4/27/2016 11:49	6001	6000	7809
9	4/27/2016 11:49	6001	6000	7810
10	4/27/2016 11:49	6000	6000	7810
11	4/27/2016 11:49	6000	6000	7811
12	4/27/2016 11:49	6000	6000	7811
13	4/27/2016 11:49	6000	6000	7811
14	4/27/2016 11:49	6000	6000	7811
15	4/27/2016 11:49	6000	6000	7813
16	4/27/2016 11:49	5999	6000	7812
17	4/27/2016 11:49	6000	6000	7813
18	4/27/2016 11:49	6000	6000	7814
19	4/27/2016 11:49	6000	6000	7813
20	4/27/2016 11:49	6000	6000	7814
21	4/27/2016 11:49	5999	6000	7813
22	4/27/2016 11:49	5999	6000	7813
23	4/27/2016 11:49	5999	6000	7814
24	4/27/2016 11:49	6004	6000	7806
25	4/27/2016 11:49	6003	6000	7808

P-Pump_1600935_1600935

Figure 3.4: A sample Excel sheet of Fluid Control Center

For the purpose of observing and documenting the bubble nucleation process, a Dino-Lite digital microscope was used. It has a magnification range of 5x-140x with 1.3 megapixel resolution. A stand was used to fix the camera position in any desired direction. Dino capture 2.0 software was used for capturing pictures and recording videos. Extended depth the field (EDOF) is one of the important features that are included with the microscope's specifications. It takes multiple pictures at different depths of field and combines them into one clear image. Its high magnifications and resolution helped to obtain good quality pictures and videos during the process of releasing pressure. It also has a refocus specification that allows focusing at different depths of the object. Figure 3.5 shows the Dino-Lite digital microscope.

Figure 3.5: Dino-Lite Digital Microscope

3.2 Wettability Alteration of Glass Surfaces

Wettability alteration techniques, that are explained in the following paragraphs, were utilized to change surface wettability and examine its effect on bubble nucleation of CO_2 from its supersaturated solution. Hydrophilic surfaces were already available since the uncoated glass vials, beads, and plates used in this study are inherently hydrophilic. For preparing hydrophobic surfaces, coating process was conducted using chemical materials that change glass substrates from hydrophilic to hydrophobic. Chlorinated polydimethylsiloxane (CM) and chlorinated fluoroalkylmethylsiloxane (CF) were used to prepare hydrophobic surfaces.

The aim of the coating was to provide a surface that has water repellency. Both chemicals contain chlorine component. The chlorine is a very active chemical component that can readily react with the hydroxyl and silanol groups on the glass surface. In addition, it can react with siliceous and oxide surfaces that offer a perfect coating and change wetting degree of the surface.

The surfaces of the hydrophobic vials will have lower surface energy compared to the uncoated vials. The typical critical surface tensions values of CM and CF coated surfaces (from the information provided by the vendor) are 25 dynes/cm and 19-16 dyne/cm, respectively.

Since the materials used for coating were a combination of corrosive chlorinated polysiloxanes, necessary safety protocols were followed while conducting coating process.

The coating process was also implemented on the glass slides of dimensions 10 mm x 10 mm and glass beads of 3 mm diameter. These glass slides carry the same specifications of the vials, which are made of borosilicate. Some of them were used for measuring contact angles, using a goniometer, and surface roughness, using an atomic force microscope (AFM), before and after the coating process. The other slides were used for measuring the surface chemistry using an X-ray photoelectron spectroscopy (XPS). These measurements can assure the success of coating process, since contact angles, surface roughness, and surface chemistry must vary before and after the coating.

Two new test tubes were used for placing glass slides, vials, or beads inside it. One of the tubes was used for formulating 10% CM in toluene solution and the other one was used for preparing 10% of CF in toluene solution. These tubes were safe to be used in this study because they do not react with the chemicals that utilized in coating process.

Firstly, the mass of empty tubes and glass sample were measured. After that, the sample was immersed in 35 g of toluene. The samples were rinsed with the toluene for 10 minutes, the toluene was discarded from both the tubes, and they were filled with toluene again. Then, the total mass (sample + bottle + toluene) was measured. Subtracting the mass of the sample and bottle from the total mass, gives the mass of fresh toluene added, according to which the mass of CM or CF is determined to prepare 10% by mass of CM or

CF solution in toluene. The contents in the tubes were mixed for 60 minutes to ensure the reaction between samples and the solution.

Table 3.1: The mass of the materials used for preparing 10% CM solution

Number	Materials used for preparing 10% by mass of CM in toluene	Weight (g)
1	Empty plastic bottle	12.285
2	Samples	19.066
3	CM	2.5588
4	Toluene	25.588
5	Plastic bottle + Samples	31.351
6	Total (samples+ bottle + toluene)	56.939

Table 3.2: The mass of the materials used for preparing 10% CF solution

Number	Materials used for preparing 10% by mass of CF in toluene	Weight (g)
1	Empty tube	12.336
2	Samples	19.603
3	CF	2.654
4	Toluene	26.54
5	Plastic bottle + Samples	31.941
6	Total (samples + bottle + toluene)	58.481

The CM or CF treated glass samples were rinsed in a 35 g of n-hexane for 10 minutes to remove unreacted CM or CF. Then the samples were rinsed in a 35 g of methanol for another 10 minutes to remove the n-hexane. The final step was drying the samples in an oven for 20 minutes at 110 ^{o}C. Some of the dried glass slides were employed for measuring contact angle, AFM, and XPS. For glass beads, only AFM measurement was conducted. The remaining vials and beads were used for bubble nucleation experiments.

3.3 Materials and chemicals

The following are the specifications of the materials and chemicals used in the wettability alteration process.

1. Aquaphobe CM (1.0 g/ml specific gravity), supplied by Gelest Inc.

2. Aquaphobe CF (1.4 g/ml specific gravity), supplied by Gelest Inc.
3. Toluene, UV reagent grade ACS, 99.7%, supplied by Pharmco-AAPER.
4. N-Hexane, UV reagent grade ACS, 99.7%, supplied by Pharmco-AAPER.
5. Methanol, Reagent grade ACS, supplied by Pharmco-AAPER.

Tables 3.1 and 3.2, present the mass of the materials used in one batch of CM and CF coating processes.

3.4 Contact Angle Measurements

Air-water contact angle data were measured using a goniometer for untreated, CF, and CM treated glass slides. A water droplet of 5 µL is placed on each surface and the photograph of the droplet was taken and used for contact angle data using the drop shape analysis method. Figure 3.6 shows the contact angle measurement device.

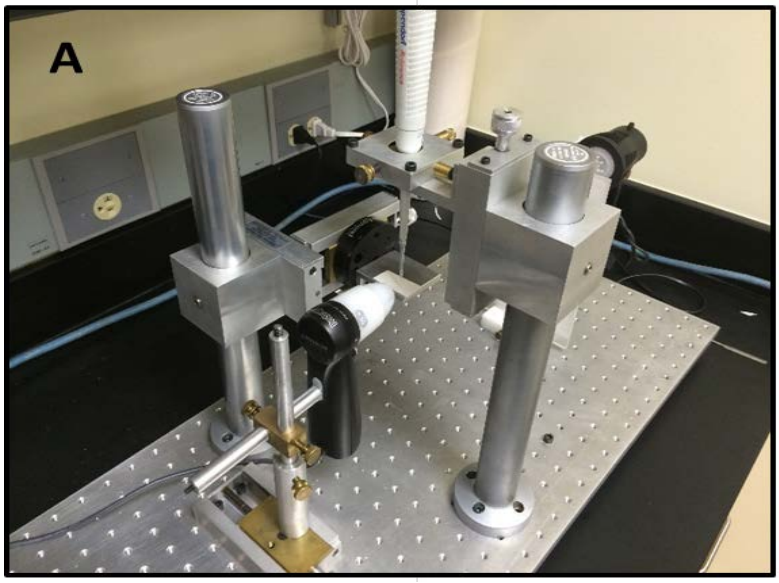

Figure 3.6: Contact angle measuring device (goniometer)

3.5 AFM Measurements

AFM measurements were conducted on hydrophilic, CM, and CF glass slides and beads to examine surface roughness before and after the coating process. The device used was Digital Instruments Nanoscope V electronics with an optical microscope for tip positioning. 2D and 3D surface topography images of the above surfaces were made before

and after the wettability alteration. Figure 3.7 it illustrates AFM device that had been utilized for the experiment.

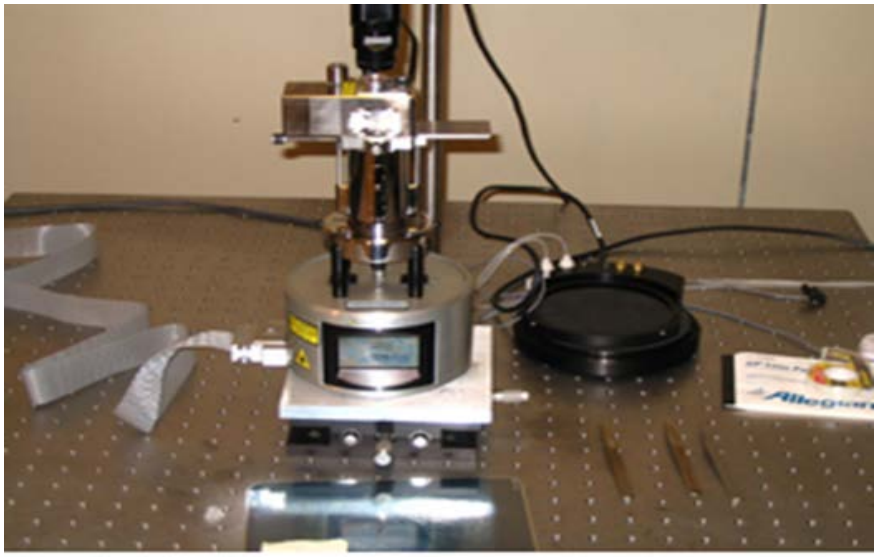

Figure 3.7: Atomic Force Microscope used for this study

3.6 XPS Measurements

The XPS facility utilized to measure surface chemistry of the substrates used in this study is shown in Figure 3.8 (a). The XPS system utilizes a precision long-stroke ultra-high vacuum (UHV) manipulator to couple the surface analysis system to a load-lock chamber. The transfer system for coupling was based on two O-ring seals differentially pumped by a 70 L/s turbo molecular pump (TMP). Another 300 L/s TMP was used for pumping load lock chamber which was initially used for evacuating the analytical chamber. A 330 L/s ion pump was responsible for maintaining vacuum in the analytical chamber and it was supplemented by a titanium sublimation pump. A nude ionization gauge was used to measure base pressure, giving a typical value of $2x10^{10}$ torr. Mg anode of a PHI 300 Watt Twin Anode X-ray source was used for XPS measurements.

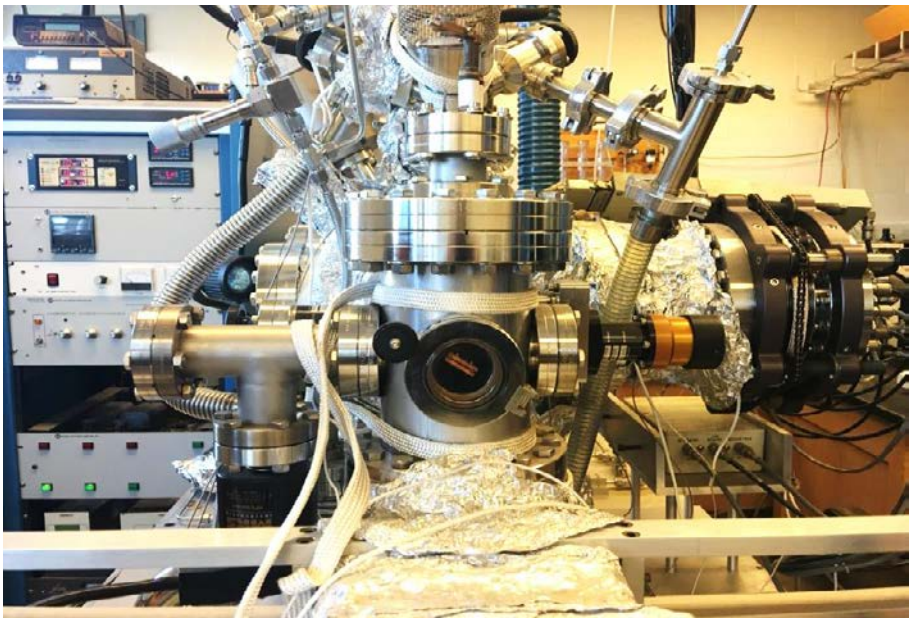

(a)

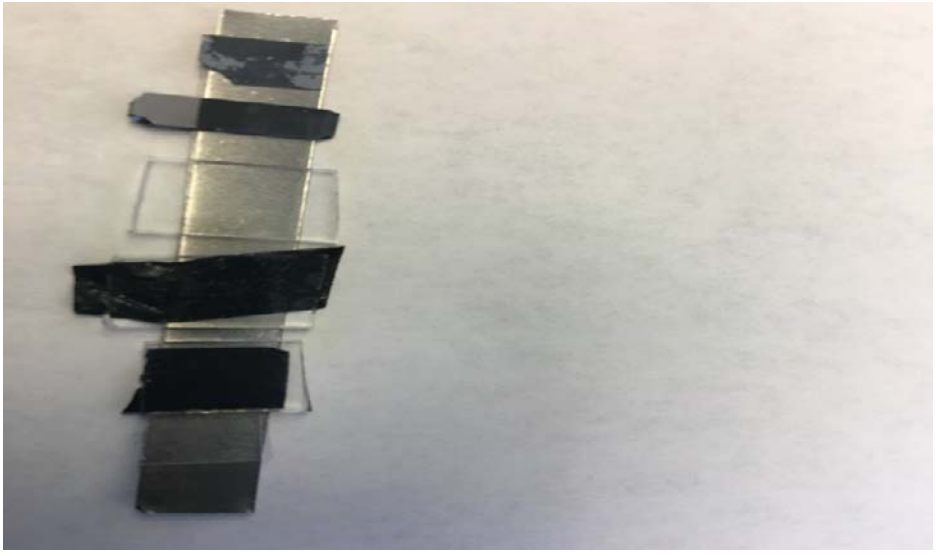

(b)

Figure 3.8: (a) XPS device; (b) Glass slides used for surface chemistry analysis

3.7 Bubble Nucleation Experiments

At the beginning of the bubble nucleation experiments, the glass vial having hydrophilic or hydrophobic surface and with or without hydrophilic or hydrophobic glass beads, was filled with deionized water to a height of 5 mm, and placed inside the pressure cell. CO_2 was injected by the P-pump to the pressure cell to flush out the trapped air for 30 minutes at 200 mbar pressure. Then the pressure cell's exit valve was closed and the CO_2 pressure was increased to 6000 mbar for saturation. Since the vial's lid inside the cell was opened, water in the vial can be saturated with CO_2. All the experiments were carried out at room temperature 25 °C.

While carrying out the experiment, three surfaces were used to study the bubble nucleation of CO_2 from its aqueous supersaturated solution. One hydrophilic and two hydrophobic surfaces (CM treated and CF treated) were used in this research. The vials utilized were cylindrical glasses which added an advantage to these experiments as vials that have any sharp edges or curves may have an effect on bubble nucleation. And hence, in this research, the effect of container shape was eliminated. No surfactants or any chemical materials were added to water as they can change the surface tension of water and/or wettability of the solid surface.

Semi-infinite diffusion equation for planar geometry was used to estimate saturation time required to saturate 5 mm height of water with CO_2.

$$\tau = \frac{Dt}{l^2} \qquad \textbf{Equation 3.1}$$

where,

$\tau =$ Dimensioless variable

$D =$ Diffusion coefficient, $\mathrm{mm}^2/\mathrm{sec}$,

$t =$ Diffusion time, sec

$l =$ Diffusion height, mm

The following parameters were used to calculate the saturation time required:

$\tau = 2$; D = 0.0016 mm^2/sec; and l = 5 mm

Based on the calculated diffusion time, CO_2 requires almost 9 hours to saturate 5 mm height of water. However, to ensure complete saturation, a 24-hour saturation time was used for the bubble nucleation experiments.

For hydrophilic vial surfaces, after the air flush out step, the procedure followed was using 6000 mbar as saturation pressure for 24 hours to saturate CO_2 in water. After the saturation time, pressure was suddenly reduced by 1000 mbar and kept constant for 15 minutes to observe any bubble nucleation. The same experiment was repeated multiple times with step-down pressures of 1000 mbar and 500 mbar also. Bubble nucleation was not observed even when the pressure was reduced to 0 mbar. However, it was observed that inserting a plastic pipette in the CO_2 supersaturated water after opening the pressure cell caused bubble nucleation.

After concluding the hydrophilic experiments, bubble nucleation experiments using the 10% CM and 10% CF coated vials were conducted. The same procedure was repeated for installing the cell, flushing out trapped air for 30 minutes by applying a 200 mbar of CO_2, and applying a 6000 mbar pressure for 24 hours of saturation time. The step-down pressure of 1000 mbar was used every 15 minutes after saturation time. When the bubble nucleation pressure was observed, a smaller step-down pressures of 500 mbar and 100 mbar were used to determine the bubble nucleation pressure more accurately.

A series of experiments were also conducted using spherical glass beads of 3 mm diameter. For all the experiments, hydrophilic vials were utilized and same aforementioned steps were followed. The aim of this part of the study was to confirm smooth hydrophilic surfaces do not promote bubble nucleation. One hydrophilic glass bead was employed for this study. One and four glass beads were used in the case of CM and CF hydrophobic surfaces.

CHAPTER IV

RESULTS AND DISCUSSION

4.1 Hydrophilic Vials

Bubble nucleation did not occur while using hydrophilic vials with a saturation time of 24 hours. Figures 4.1 (a), (b), and (c) show hydrophilic vial after the saturation time (i.e. before releasing pressure), at zero mbar step-down pressure, and at the time of inserting a plastic lab pipette after opening the cell's lid respectively.

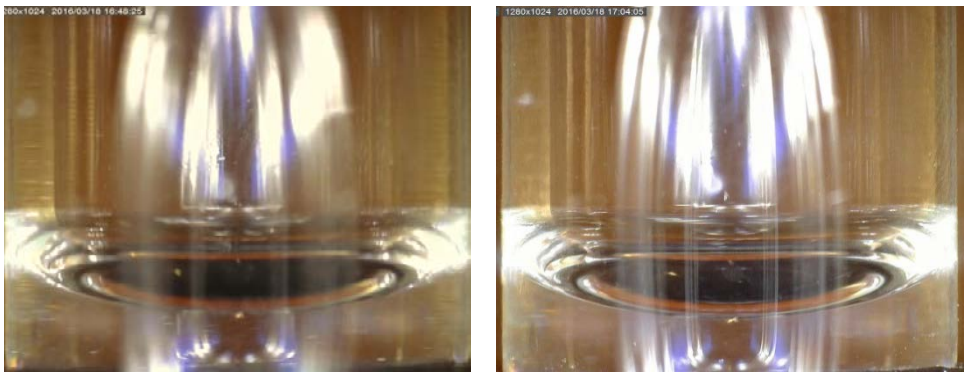

(a) (b)

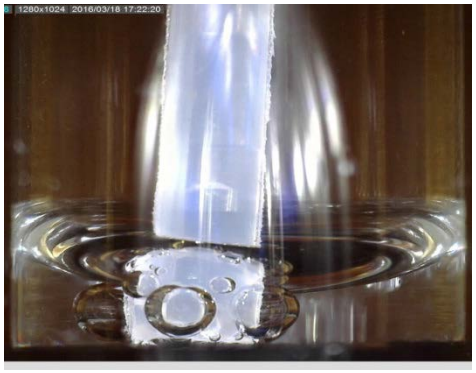

(c)

Figure 4.1: Hydrophilic vial (a) after 24-hour saturation time at 6000 mbar; (b) at zero mbar step-down pressure; and (c) while inserting the plastic tube

Water molecules strongly wet hydrophilic borosilicate glass due to which it may be difficult to promote gas bubble nucleation on these surfaces even at the highest supersaturation levels (from 6000 mbar to 0 mbar) used in this study. Inserting a plastic tube created new low energy sites for bubble nucleation and encouraged gas bubble nucleation. Also, the presence of the potential pre-existing gas might have played a role in bubble nucleation.

The same plastic tube that was used to insert into the saturated liquid vial from the previous experiment was utilized with another new vial that filled with distilled unsaturated water. This step was done to check if there will be any bubbles formed around the plastic tube or not. The process did not show any bubble nucleation around the plastic tube, which confirms that the bubbles formed around plastic tube in the previous test was CO_2 gas bubbles and not air bubbles.

4.2 Hydrophobic Vials

Both the CM and CF treated vials resulted CO_2 gas bubble nucleation from the water. Changing surface wettability towards hydrophobic nature promoted bubble nucleation and it may be due to the air or CO_2 trapped at the solid-liquid surface or the cohesive forces between the water and hydrophobic force might become weakened and ruptured (Ryan and Hemmingsen (1993&1998). This type of mechanism could be used for gas-liquid separations. Although bubble nucleation occurred in both the CM and CF coated vials, bubble nucleation occurred at different values of step-down pressures. Figure 4.2 presents the starting pressures of gas bubble nucleation for CM and CF coated vials, respectively. Figure 4.3 shows the average starting pressure and the standard deviation for gas bubble nucleation in CM and CF treated vials, respectively.

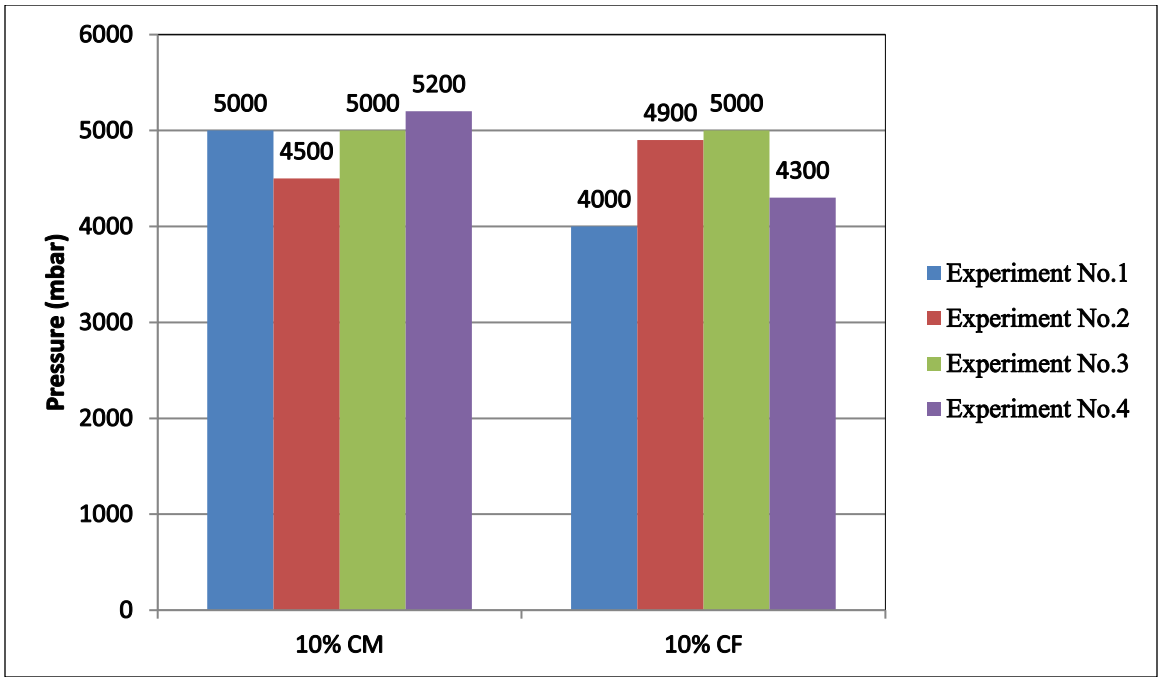

Figure 4.2: Starting pressures for gas bubble nucleation in CM and CF treated vials

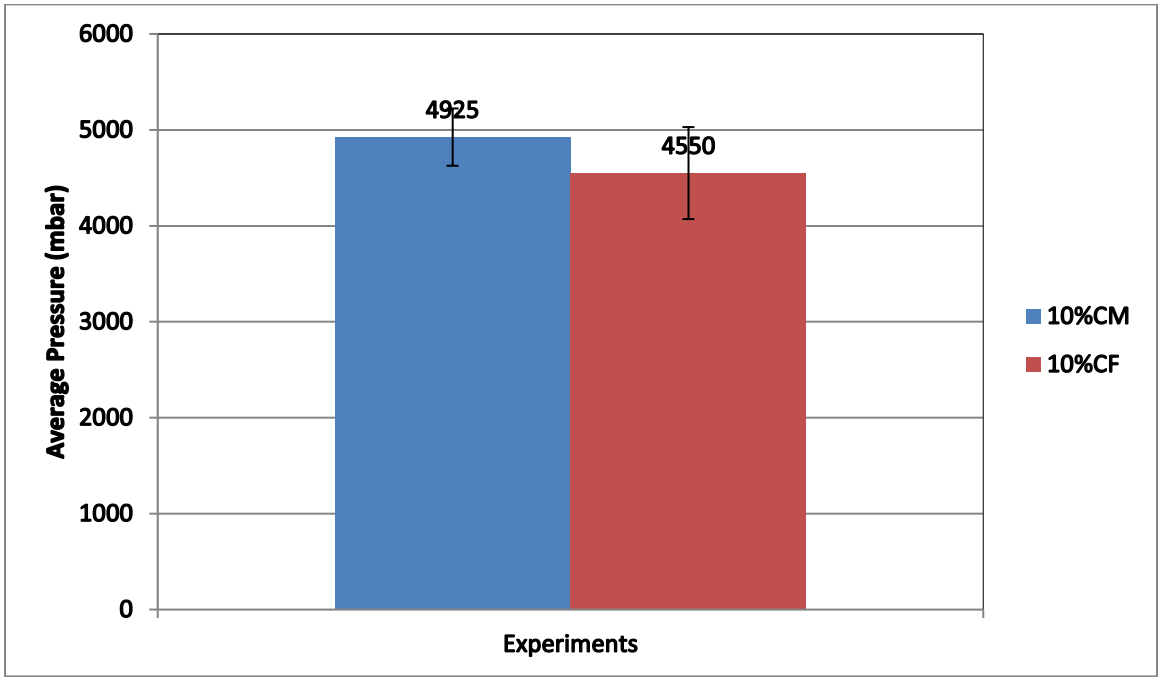

Figure 4.3: Average gas bubble nucleation starting pressures and their standard deviation for CM and CF treated vials

As shown in figure 4.3, average starting pressure for gas bubble nucleation in CM treated vials was 4925 mbar and the standard deviation was 298.6 mbar. Whereas, for CF treated vials the average starting pressure for gas bubble nucleation was 4550 mbar and its standard deviation was 479.6 mbar.

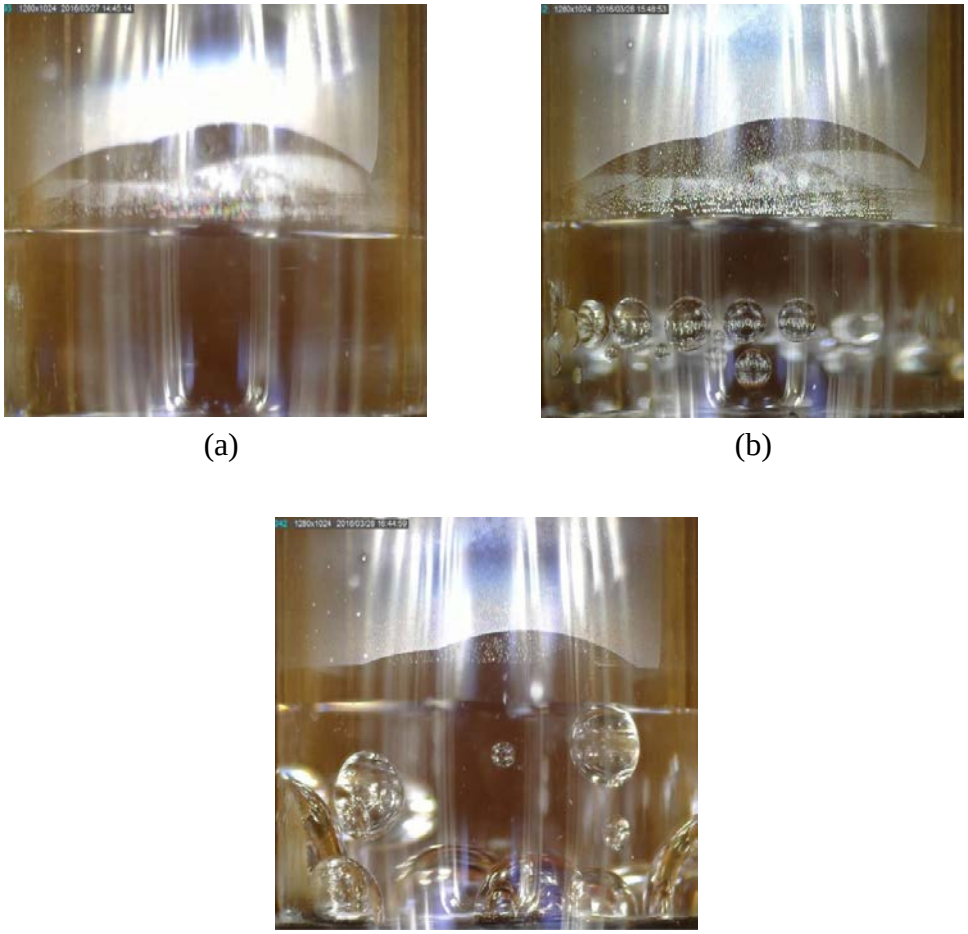

(a) (b)

(c)

Figure 4.4: CM coated vial (a) after 24-hour saturation time at 6000 mbar; (b) at the beginning of bubble nucleation, 4000 mbar; and (c) at zero mbar

For hydrophobic vials, using saturation time of 24 hours showed gas bubble nucleation while step-down pressure process. Figures 4.4 (a), (b), and (c) show the CM coated vial after saturation time, at the initiation of bubble nucleation, and at zero mbar pressure. Figures 4.5 (a), (b), and (c) are the corresponding figures for CF coated vial.

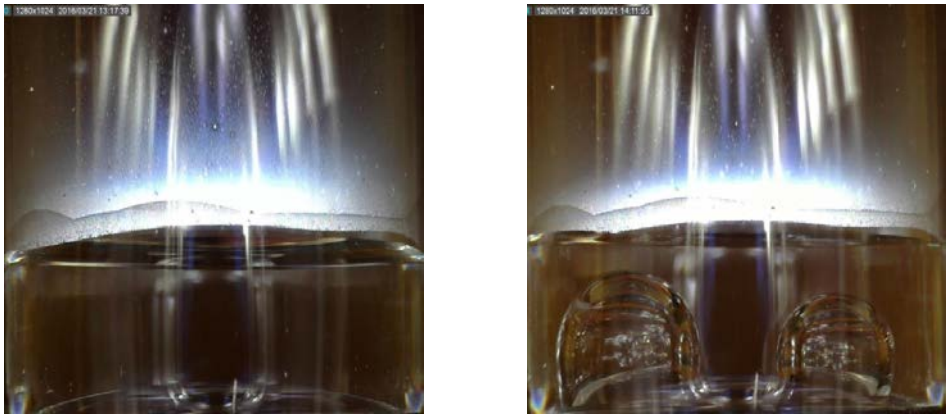

(a) (b)

(c)

Figure 4.5: CF coated vial (a) after 24-hour saturation time at 6000 mbar; (b) at the beginning of bubble nucleation, 2000 mbar; and (c) at zero mbar

From the above figures, it can be observed that bubble nucleation is promoted by using hydrophobic surfaces (CM and CF vials).

4.3 Contact Angles Measurement Results

The Figures 4.6 (a), (b), and (c) below present the contact angles measurement for untreated glass slide, CM glass slide, and CF glass slide, respectively.

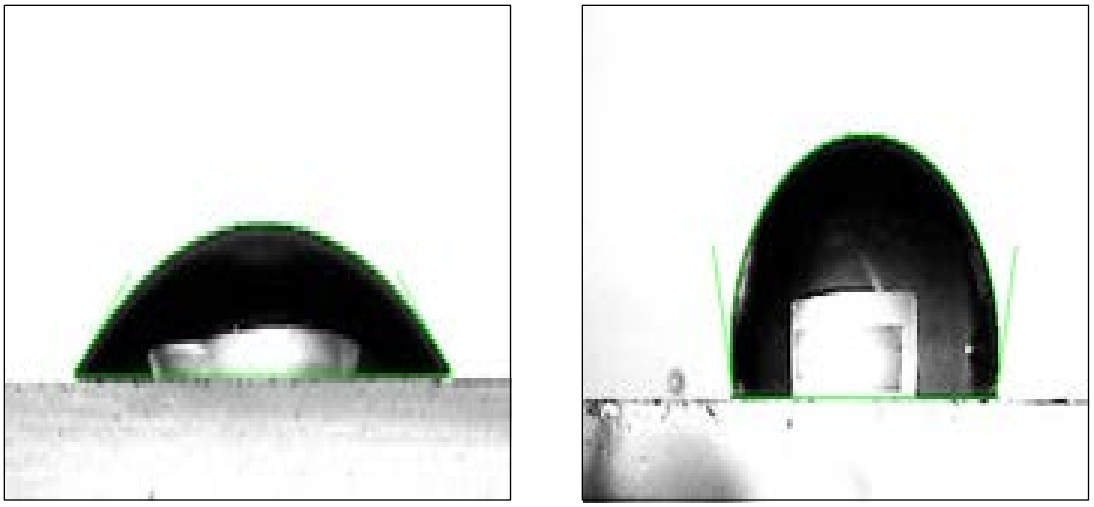

(a) (b)

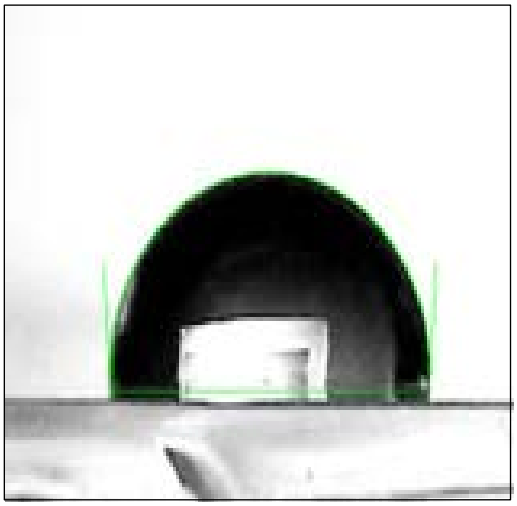

(c)

Figure 4.6: Air-water contact angle measurement (a) Untreated glass slide, 38.7^{o}; (b) CM treated glass,102^{o}; and (c) CF treated glass slide, 94.3^{o}

Average contact angle and its standard deviation data for the hydrophilic and hydrophobic samples are shown in figure 4.7.

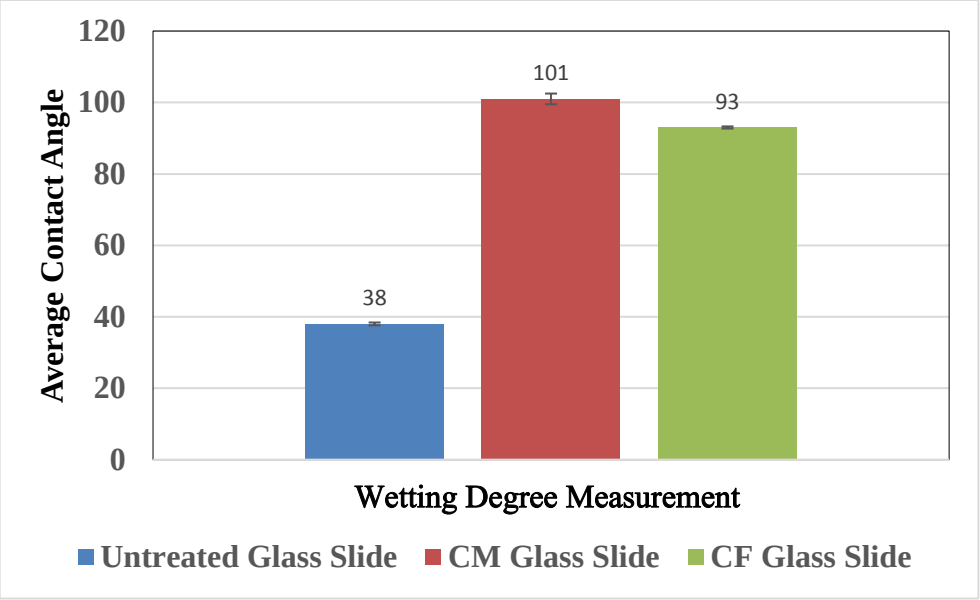

Figure 4.7: Average air-water contact angle and standard deviation data of untreated (hydrophilic) and treated (hydrophobic) surfaces

The average air-water contact angle for untreated glass sample was 38^{o} and the standard deviation was 0.4^{o}. For CM sample, the corresponding data were 102^{o} and 1.5^{o}, for CF they were 93^{o} and 0.3^{o}. Contact angle values can characterize the wettability degree of the glass surface using water as a liquid phase on clean solid surface. From the obtained measurements, it can be clearly seen the average difference between contact angle values before and after the coating process. Contact angles values increased by nearly 60^{o} after the coating process. CM treated samples showed higher values for contact angles than CF treated samples.

4.4 AFM Measurement Results

Figures 4.8 (a) and (b) show the 2D and 3D topography images obtained from AFM measurement for uncoated glass slide, respectively. Figures 4.9 (a) and (b) are the corresponding figures for CM glass slide. Figures 4.10 (a) and (b) shows the 2D and 3D topography images for CF glass slide, respectively.

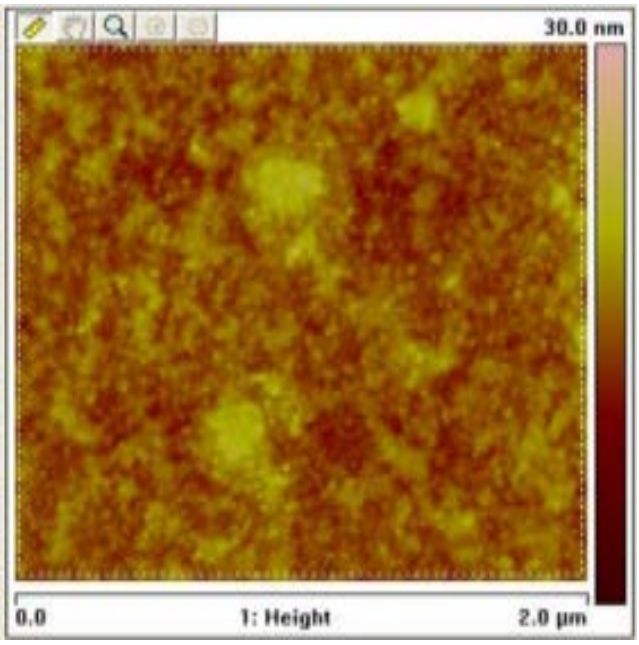

(a)

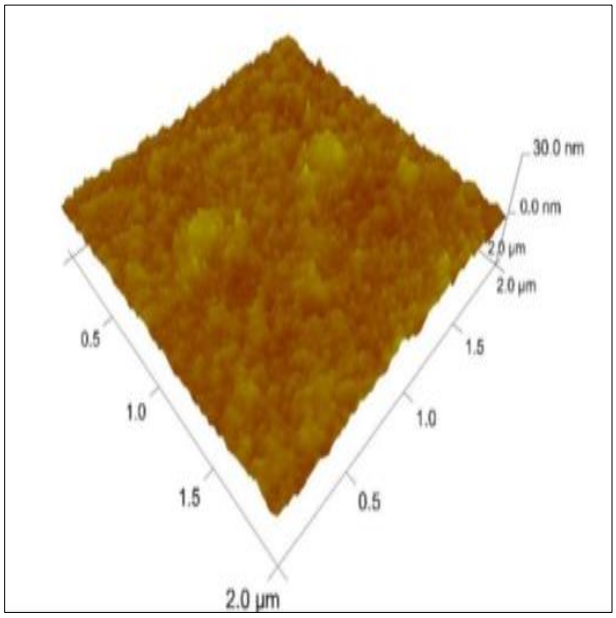

(b)

Figure 4.8: (a) 2D surface topography; (b) 3D surface topography of uncoated glass slide surface

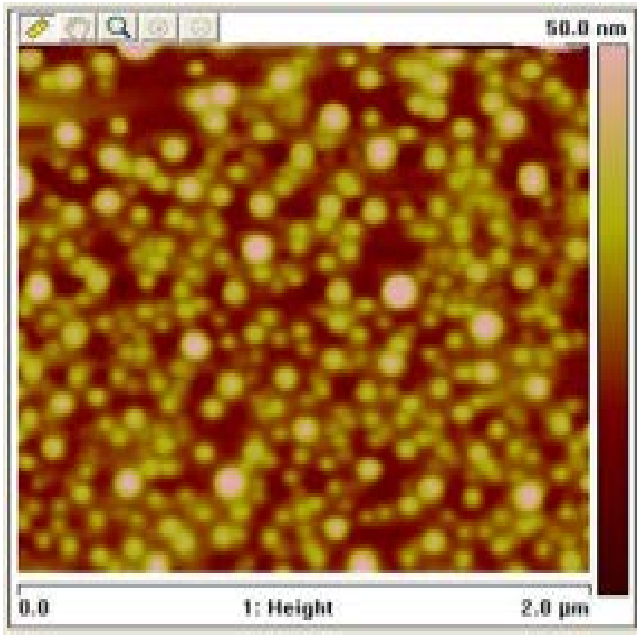

(a)

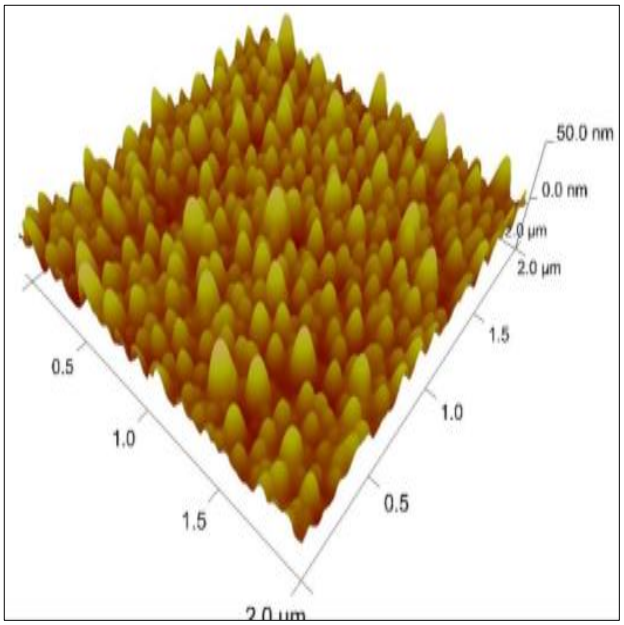

(b)

Figure 4.9: (a) 2D surface topography; (b) 3D surface topography of CM glass slide surface

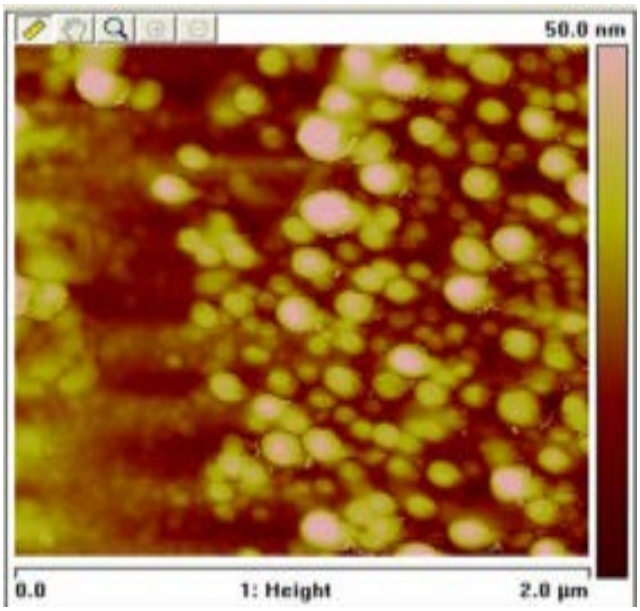

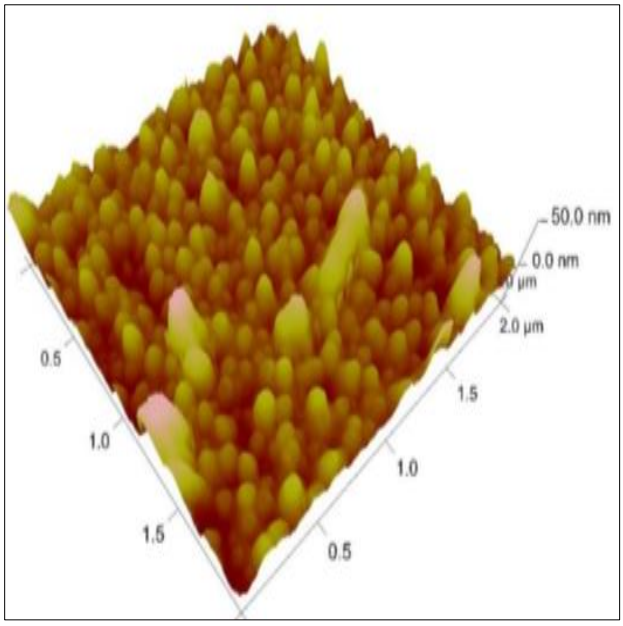

(b)

Figure 4.10: (a) 2D surface topography; (b) 3D surface topography of CF glass slide surface

The reported AFM roughness measurements are of average roughness (Ra) defined as in equation 4.1 (De Oliveira, 2012). This parameter is used to compare the surface roughness values of the three measured samples.

$$\boldsymbol{Ra = \frac{1}{L} \int_o^L Z(x)\, dx} \qquad \textbf{Equation 4.1}$$

where,

$Ra =$ roughness average

$L =$ sample length

$Z =$ the profile of the surface

$x =$ the measurement position

Uncoated glass slide had the lowest value of Ra, which was 1.48 nm, whereas the Ra for CM glass slide was 5.71 nm and Ra for CF was 7.10 nm, which was the highest value.

4.5 XPS Measurement Results

Figures 4.11 (a), (b), and (c) show the XPS results for uncoated slide, CM coated and CF coated glass slides, respectively.

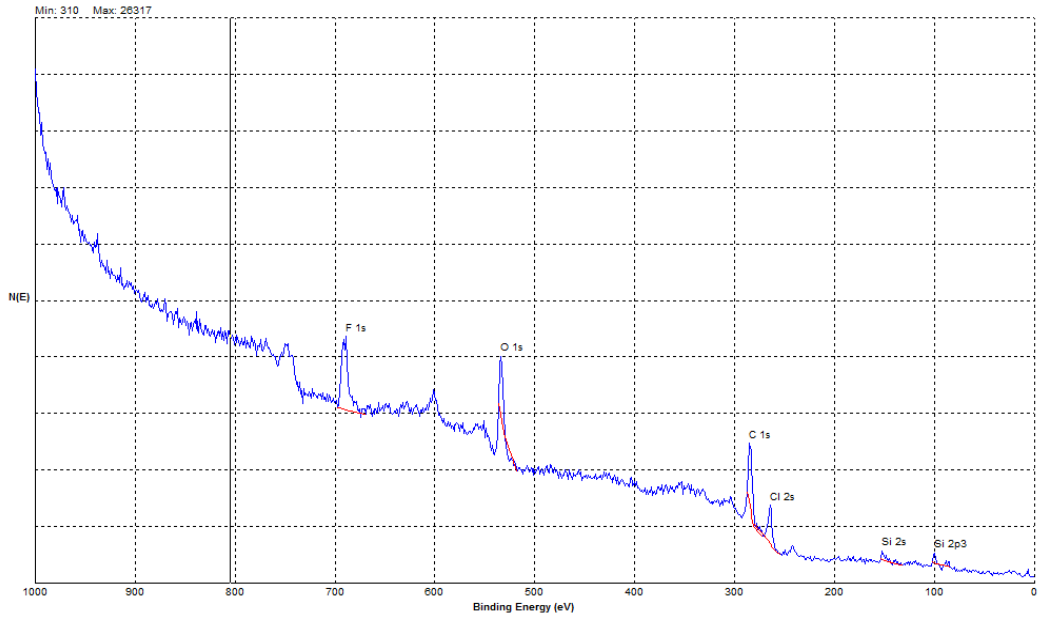

(a)

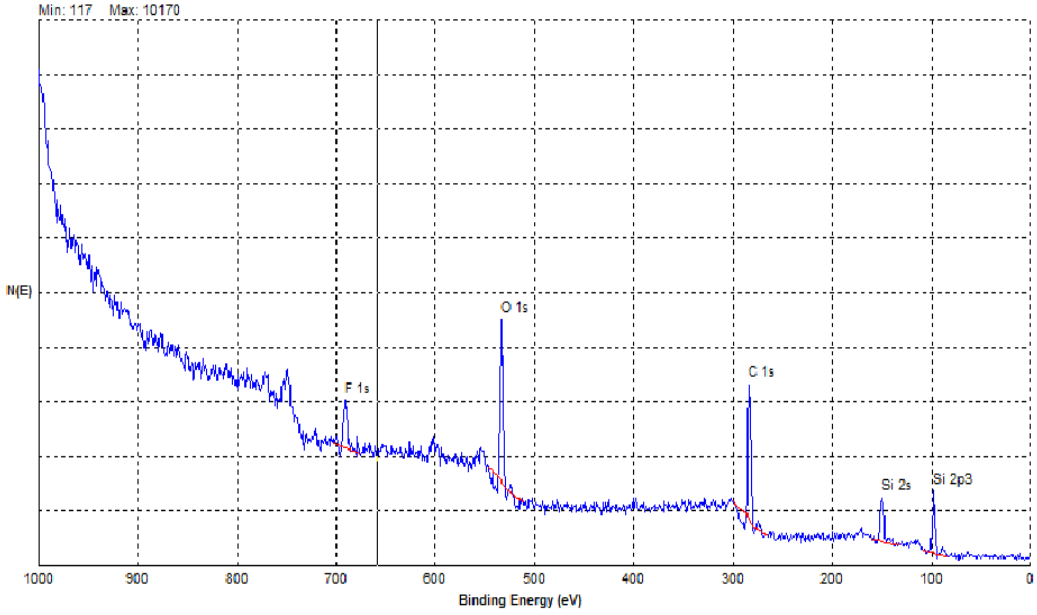

(b)

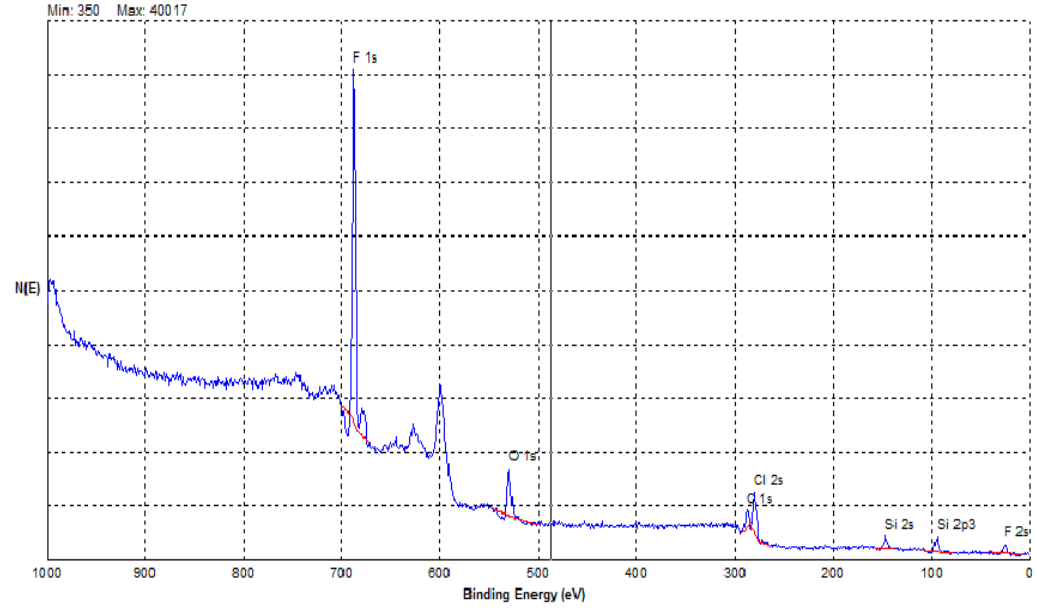

(c)

Figure 4.11: XPS results for (a) uncoated glass slide; (b) CM coated glass slide; and (c) CF coated glass slide

Uncoated and CM glass slides might be contaminated by fluorine from CF glass slide while conducting XPS surface chemistry measurement. For these measurements, samples prior to washing in n-hexane and methanol were used.

It can be observed from Figure 4.11 (a) that untreated slide contains silicon, oxygen, chlorine, and carbon. For CM slide (Figure 4.11 (b)), higher amounts of oxygen carbon, silicon, and oxygen can be observed. Whereas in the case of CF slide (Figure 4.11 (b)), higher amount of fluorine and smaller amount of silicone and chlorine can be found.

4.6 Glass Beads Results

Glass beads of 3 mm diameter coated with 10% CM and CF were used for experiments using hydrophilic vials. Using one hydrophilic glass bead during saturating time, indicated no bubble nucleation even when the step-down pressure was reduced to zero mbar. Utilizing one or four glass beads of both CM and CF showed bubble nucleation occurrence during the step-down pressures.

Utilizing spherical hydrophobic coated glass beads promoted bubble nucleation and confirmed the ability of wettability alteration effect on promoting gas bubble nucleation. Figures 4.12 (a), (b), and (c) illustrate hydrophilic vial with one hydrophilic glass bead after the 24-hour saturation time at 6000 mbar, zero mbar pressure, and at the time of inserting a plastic tube.

Figures 4.13 (a), (b) and (c) show hydrophilic vial that contained one coated CM glass bead after the 24-hour saturation time at 6000 mbar, at the initiation of bubble nucleation during the step-down pressure to 1000 mbar, and at zero mbar. Figures 4.14 (a), (b), and (c) show the corresponding figures for CF coated glass bead. It may be noted that the bubble nucleation occurred at 5000 mbar.

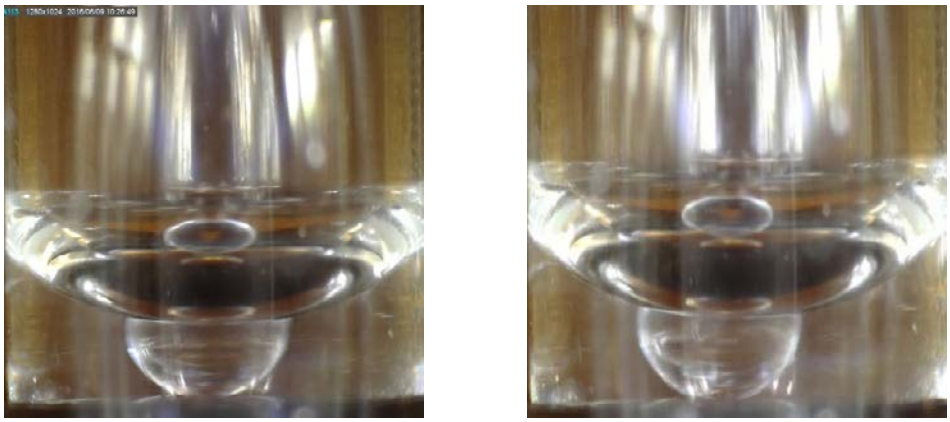

(a) (b)

(c)

Figure 4.12: Hydrophilic vial with one hydrophilic glass bead (a) after saturation time; (b) at zero mbar; and (c) at the time of inserting a plastic tube

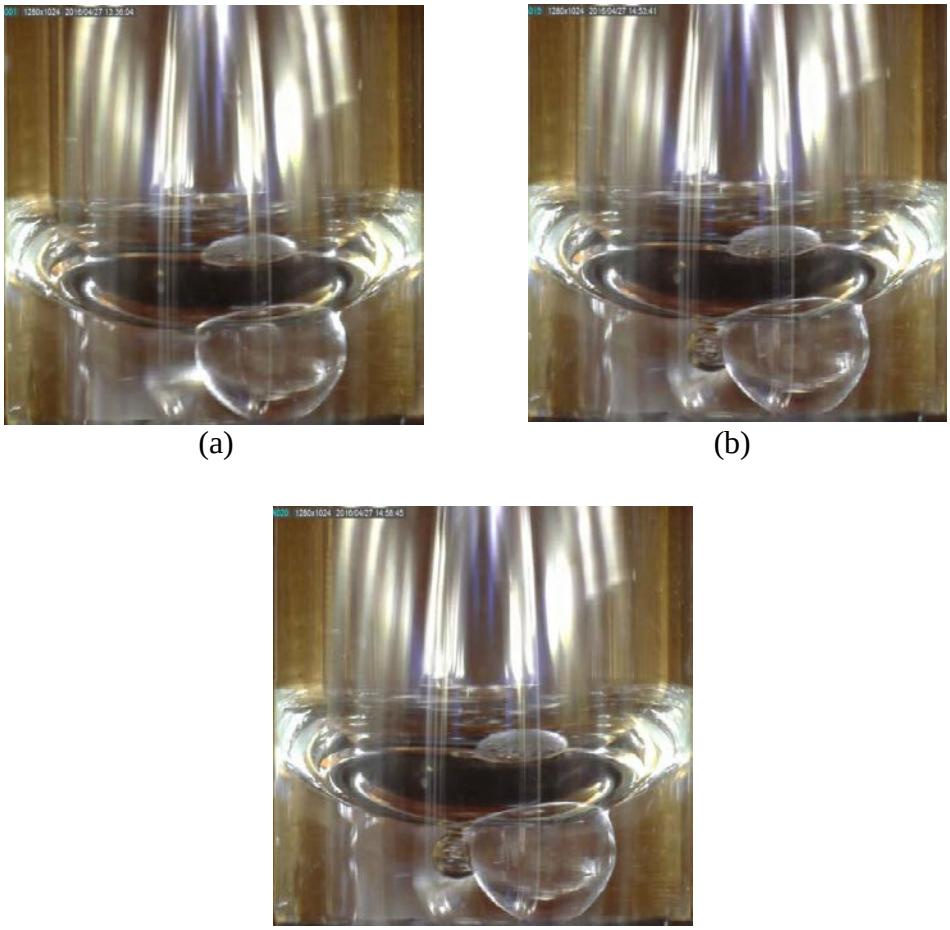

(a) (b)

(c)

Figure 4.13: Hydrophilic vial contained one coated CM glass bead (a) after 24-hour saturation time at 6000 mbar; (b) at the beginning of bubble nucleation at 1000 mbar; and (c) zero mbar

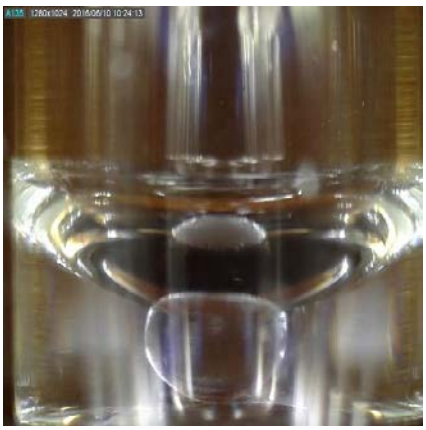

(a)

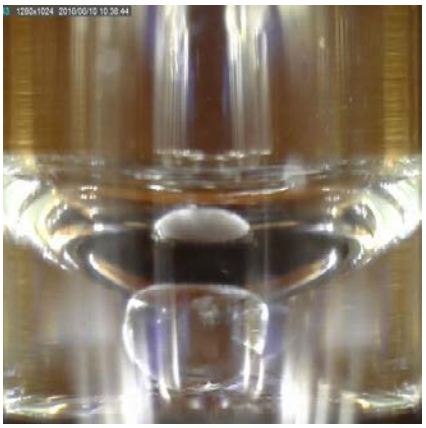

(b)

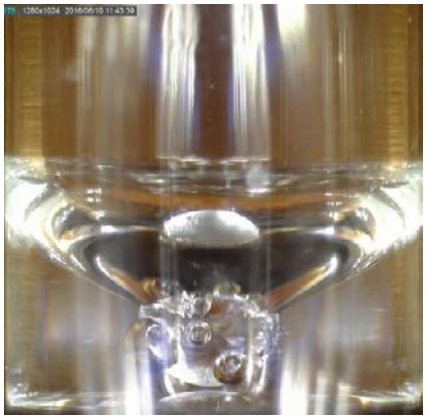

(c)

Figure 4.14: Hydrophilic vial contained one coated CM glass bead (a) after 24-hour saturation time at 6000 mbar; (b) at the beginning of bubble nucleation at 5000 mbar; and (c) zero mbar

Using four CM and CF treated glass beads each in hydrophilic vials encouraged bubble nucleation. Figures 4.15 (a), (b), and (c), show hydrophilic vials that contained four CM coated glass beads after 24-hour saturation time at 6000 mbar, at the beginning of bubble nucleation at 5000 mbar, and at zero mbar pressure. Figures 4.16 (a), (b), and (c) show the corresponding images for CF coated glass beads.

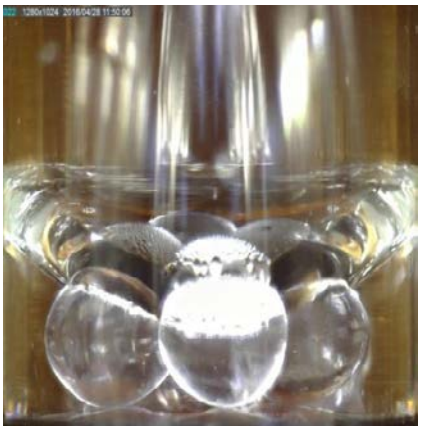

(a)

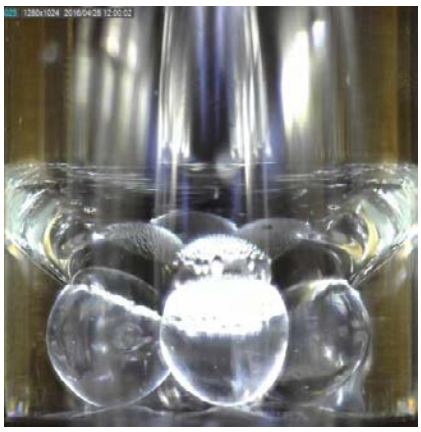

(b)

(c)

Figure 4.15: Hydrophilic vial containing four coated CM glass beads (a) after 24-hour saturation time at 6000 mbar; (b) at the beginning of bubble nucleation at 5000 mbar; and (c) zero mbar

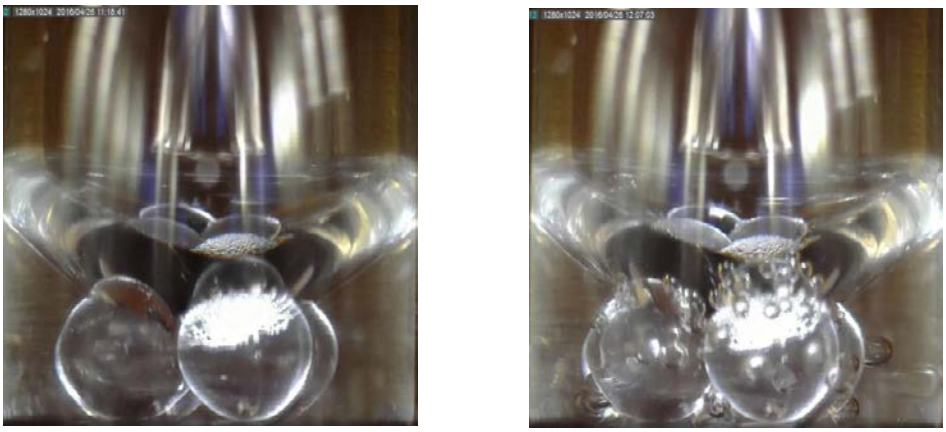

(a) (b)

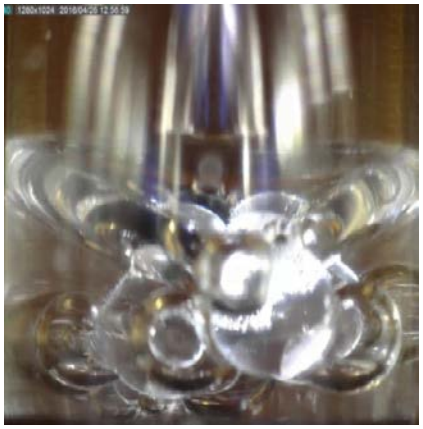

(c)

Figure 4.16: Hydrophilic vial containing four coated CM glass beads (a) after 24-hour saturation time at 6000 mbar; (b) at the beginning of bubble nucleation at 4000 mbar; and (c) zero mbar

Figures 4.17 (a) and (b) show 2D and 3D show surface topography images of untreated glass bead, respectively. Figures 4.18 (a) and (b) show the corresponding images for CM treated glass bead and figures 4.19 (a) and (b) show the corresponding images for CF glass bead.

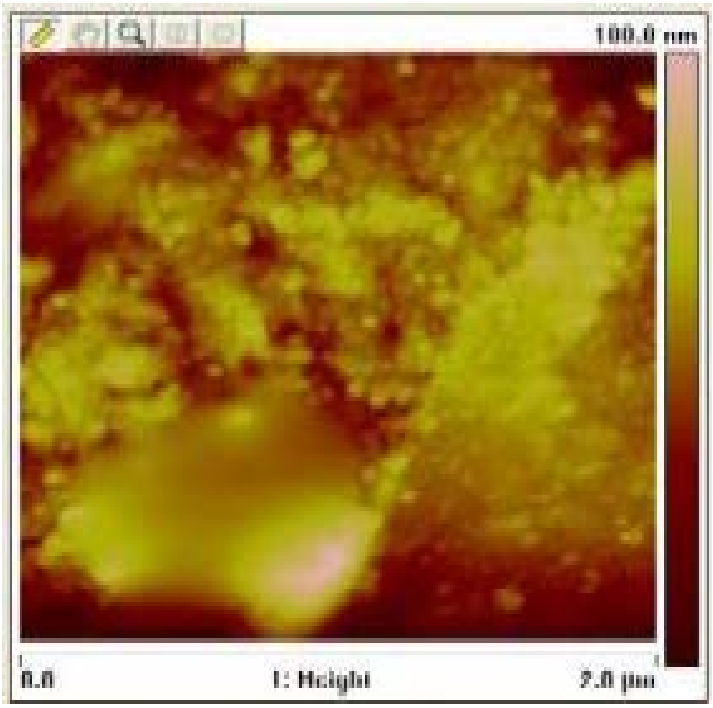

(a)

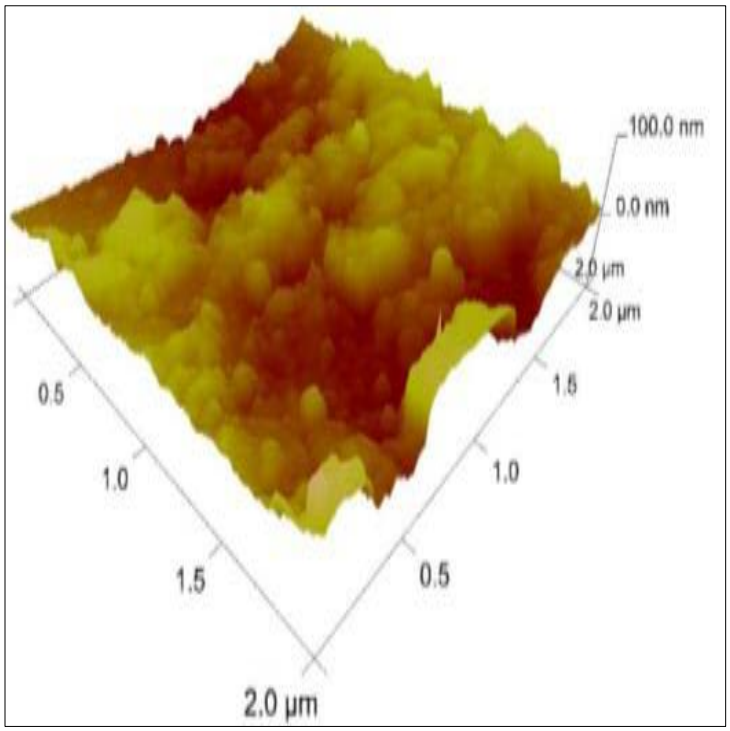

(b)

Figure 4.17: (a) 2D; and (b) 3D topography images of untreated glass bead surface

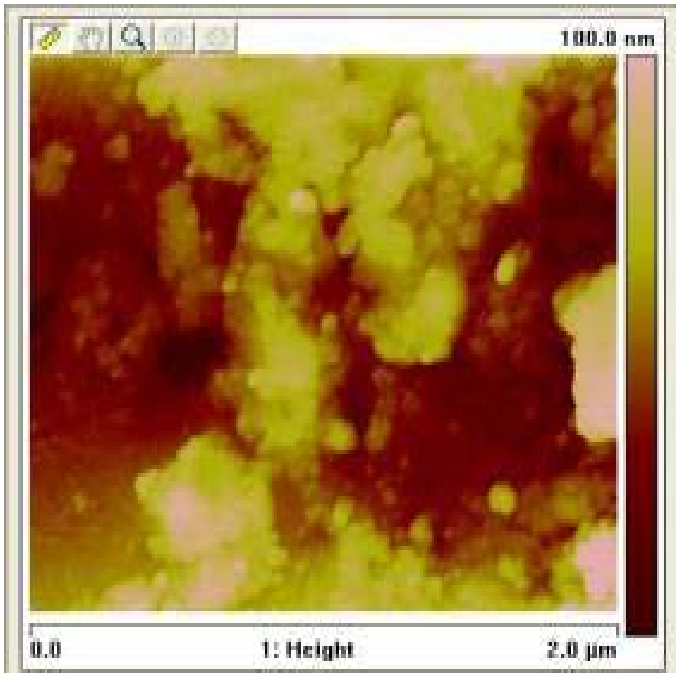

(a)

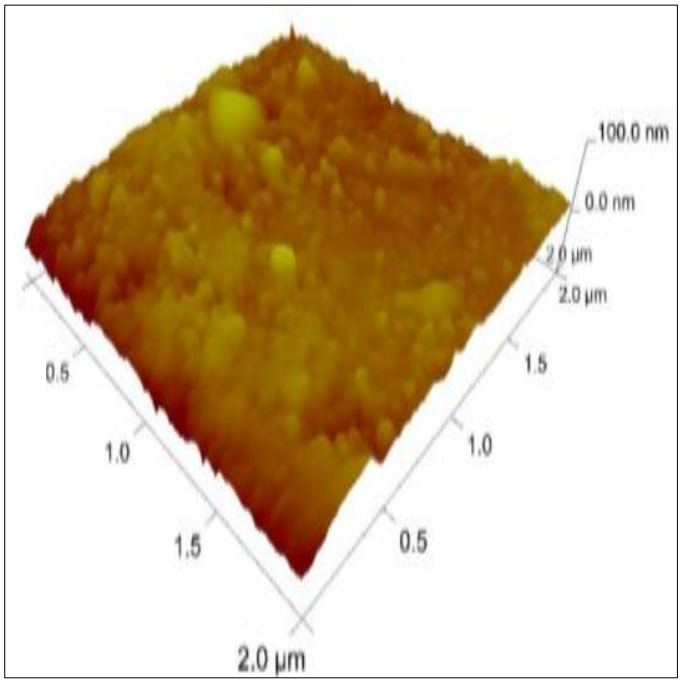

(b)

Figure 4.18: (a) 2D; and (b) 3D topography images of CM treated glass bead surface

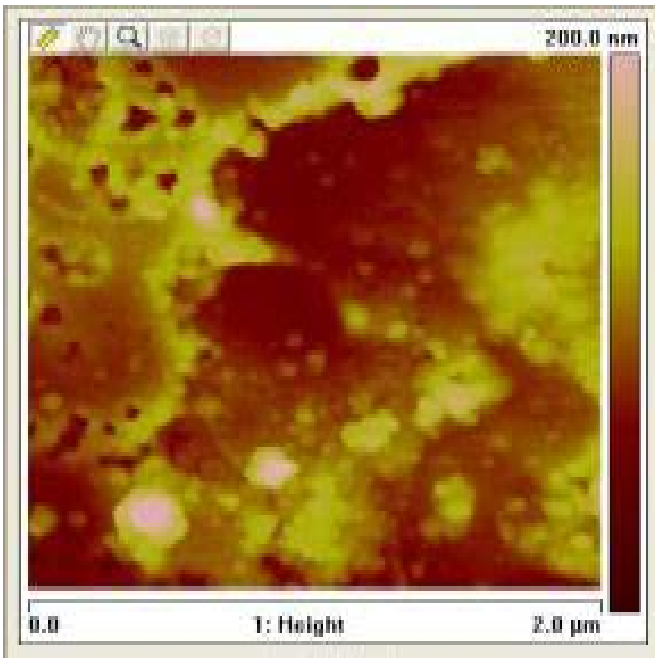

(a)

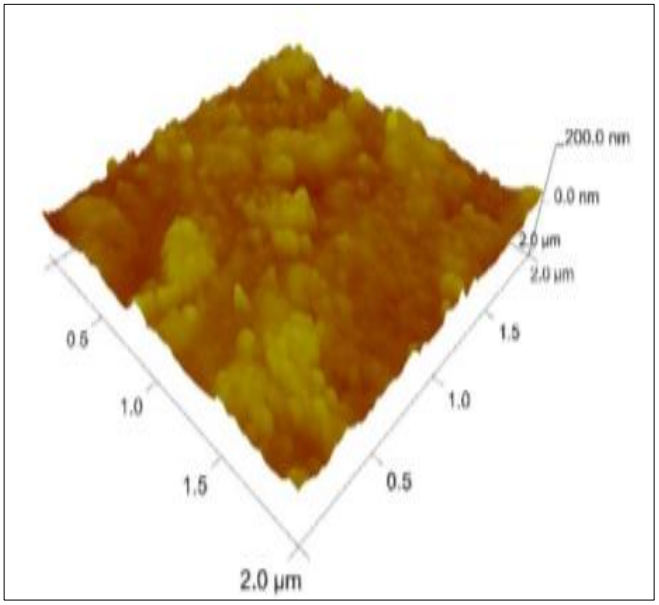

(b)

Figure 4.19: (a) 2D; and (b) 3D topography images of CF treated glass bead surface

Based on AFM measurements, average roughness (Ra) was found to be 11.7, 17.9, and 22.1 nm for untreated, CM and CF treated glass beads, respectively. Therefore, CF glass bead had the highest Ra.

CHAPTER V

CONCLUSIONS AND RECOMMENDATIONS

Gas bubble nucleation and liberation from liquids take place in many natural and industrial processes, especially, in the oil and gas production process. Bubble nucleation is the first step of the dissolved gas separation. Most of the times, bubble nucleation occurs on the solid wall of the vessel that contains the liquid and/or any solid particles and/or structures in the vessel. Hence, it is required to investigate solid surfaces and surface wettability in order to explore the factors that may affect bubble nucleation formation. In recent days, using wettability alteration technique has played a big role in many different fields, including oil-gas industry. Therefore, it may be useful to investigate this technique on CO_2 bubble nucleation from water. Hence, the objective of this research was to conduct laboratory experiments to find the influence of wettability on bubble nucleation from supersaturated liquids.

CO_2 and water were used as the gas and liquid phases, respectively. One hydrophilic surface and two surfaces hydrophobic surfaces with different air-water contact angles were used as solid surfaces. The hydrophobic surfaces were prepared using surface chemistry alteration of glass substrates using CF (chlorinated fluoroalkylmethylsiloxane) and CM (chlorinated polydimethylsiloxane). A new facility was built to provide high level of supersaturation solution and to control pressure step-down process. The wetting degree, surface roughness, and surface chemistry for coated and uncoated samples were measured using contact angle, AFM, and XPS measurements respectively. Several experiments were conducted using hydrophilic vials, hydrophobic vials, hydrophilic glass beads, and hydrophobic glass beads to study the influence of wettability on gas bubble nucleation from a liquid. Based on the findings of this research, the following conclusions were made:

- Wettability alteration technique has great influence on bubble nucleation of gas from liquid. This technique may be useful for separating gases from saturated liquid systems.
- Providing a pulseless and continuous pressurized CO_2 to the cell using a microfluidic P-Pump was helpful to obtain accurate data.
- Untreated glass beads in water in hydrophilic vial showed no bubble nucleation even with 24-hour saturation time at 6000 mbar. However, inserting a plastic tube, a CM treated glass bead, or a CF treated glass bead after opening cell's lid caused bubble nucleation.
- Using contact angle measurement, AFM, and XPS measurements showed the efficiency of the coating process for both glass vials and glass beads.
- The average of air-water contact angle of CM coated substrate was 101^o with a standard deviation of 1.5^o and the average of air-water contact angle of CF coated substrate was 93^o with a standard deviation of 0.3^o.
- The average bubble nucleation starting pressure for CM treated glass vials was 4925 mbar with a standard deviation of 298.6 mbar and the corresponding values for CF treated glass vials were 4550 mbar and 479.6 mbar.
- Utilizing hydrophilic glass beads inside hydrophilic vials confirmed that smooth hydrophilic surfaces do not cause bubble nucleation. Whereas using hydrophobic glass beads confirmed the influence of wettability alteration for enhancing bubble nucleation.

Recommendations:

Based on this research the following recommendations are made:

- More investigations are required to determine the effect of surface wettability and roughness influence on the process of bubble nucleation and liberation.
- Coating process can be conducted on solid surfaces using different percentages of coated materials to find out the lowest percentage of the coating that would change surface wetting and enhance bubble nucleation.

- It is recommended to utilize other liquid and gas combinations to investigate the effect of wettability alteration on bubble nucleation.

REFERENCES

Abe, A. A. (2005). Abe, A. A. (2005). *Relative permeability and wettability implications of dilute surfactants at reservoir conditions* (Doctoral dissertation, Idaho State University, Idaho, USA).

Anderson, W. (1986). Wettability literature survey-part 2: Wettability measurement. *Journal of Petroleum Technology, 38*(11), 1,246-241,262.

Anisimov, M. P., Fominykh, E. G., Akimov, S. V., & Hopke, P. K. (2009). Vapor–gas/liquid nucleation experiments: A review of the challenges. *Journal of Aerosol Science, 40*(9), 733-746.

Attinger, D., Frankiewicz, C., Betz, A. R., Schutzius, T. M., Ganguly, R., Das, A., Megaridis, C. M. (2014). Surface engineering for phase change heat transfer: A review. *MRS Energy & Sustainability, 1*, E4.

Bagheri, A., Fazli, M., & Bakhshaei, M. (2016). Effect of temperature and composition on the surface tension and surface properties of binary mixtures containing DMSO and short chain alcohols. *The Journal of Chemical Thermodynamics, 101*, 236-244.

Barati-Harooni, A., Soleymanzadeh, A., Tatar, A., Najafi-Marghmaleki, A., Samadi, S. J., Yari, A., Mohammadi, A. H. (2016). Experimental and modeling studies on the effects of temperature, pressure and brine salinity on interfacial tension in live oil-brine systems. *Journal of Molecular Liquids, 219*, 985-993.

Bhushan, B., Jung, Y. C., & Koch, K. (2009). Self-cleaning efficiency of artificial superhydrophobic surfaces. *Langmuir, 25*(5), 3240-3248.

Bico, J., Thiele, U., & Quéré, D. (2002). Wetting of textured surfaces. *Colloids and Surfaces A: Physicochemical and Engineering Aspects, 206*(1), 41-46.

Bikkina, P. K. (2011). Contact angle measurements of CO_2–water–quartz/calcite systems in the perspective of carbon sequestration. *International Journal of Greenhouse Gas Control, 5*(5), 1259-1271.

Bikkina, P. K., Shoham, O., & Uppaluri, R. (2011). Equilibrated interfacial tension data of the CO2–water system at high pressures and moderate temperatures. *Journal of Chemical & Engineering Data, 56*(10), 3725-3733.

Blander, M., & Katz, J. L. (1975). Bubble nucleation in liquids. *AIChE Journal, 21*(5), 833-848.

Cashman, K. V., Mangan, M. T., & Newman, S. (1994). Surface degassing and modifications to vesicle size distributions in active basalt flows. *Journal of volcanology and geothermal research, 61*(1), 45-68.

Coffey, T. S. (2008). Diet Coke and Mentos: What is really behind this physical reaction? *American Journal of Physics, 76*(6), 551-557.

Criollo, S. A. (2011). Water and surfactant flooding at different wettability conditions.

Cyr, D. R. (2001). Bubble growth behavior in supersaturated liquid solutions.

De Oliveira, R., Albuquerque, D., Leite, F., Yamaji, F., & Cruz, T. (2012). *Measurement of the nanoscale roughness by atomic force microscopy: basic principles and applications*: INTECH Open Access Publisher.

Dean, R. B. (1944). The formation of bubbles. *Journal of Applied Physics, 15*(5), 446-451.

Delale, C. F., Hruby, J., & Marsik, F. (2003). Homogeneous bubble nucleation in liquids: The classical theory revisited. *The Journal of chemical physics, 118*(2), 792-806.

Ducker, W. A., Senden, T. J., & Pashley, R. M. (1992). Measurement of forces in liquids using a force microscope. *Langmuir, 8*(7), 1831-1836.

Espinoza, D. N., & Santamarina, J. C. (2010). Water-CO_2-mineral systems: Interfacial tension, contact angle, and diffusion—Implications to CO_2 geological storage. *Water resources research, 46*(7).

Frank, X., Dietrich, N., Wu, J., Barraud, R., & Li, H. Z. (2007). Bubble nucleation and growth in fluids. *Chemical Engineering Science, 62*(24), 7090-7097.

Frenkel′, I. A. I. i. (1955). *Kinetic theory of liquids*: Dover Publications.

Fsadni, A., Ge, Y., & Lamers, A. (2012). Bubble nucleation on the surface of the primary heat exchanger in a domestic central heating system. *Applied Thermal Engineering, 45*, 24-32.

Harvey, E. N., Barnes, D., McElroy, W. D., Whiteley, A., Pease, D., & Cooper, K. (1944). Bubble formation in animals. I. Physical factors. *Journal of Cellular and Comparative Physiology, 24*(1), 1-22.

Harvey, E. N., McElroy, W. D., & Whiteley, A. (1947). On cavity formation in water. *Journal of Applied Physics, 18*(2), 162-172.

Harvey, E. N., Whiteley, A., McElroy, W., Pease, D., & Barnes, D. (1944). Bubble formation in animals. II. Gas nuclei and their distribution in blood and tissues. *Journal of Cellular and Comparative Physiology, 24*(1), 23-34.

Hey, M., Hilton, A., & Bee, R. (1994). The formation and growth of carbon dioxide gas bubbles from supersaturated aqueous solutions. *Food chemistry, 51*(4), 349-357.

Hikita, H., & Konishi, Y. (1984). Desorption of carbon dioxide from supersaturated water in an agitated vessel. *AIChE Journal, 30*(6), 945-951.

Hua, S. Z., Sachs, F., Yang, D. X., & Chopra, H. D. (2002). Microfluidic actuation using electrochemically generated bubbles. *Analytical chemistry*, *74*(24), 6392-6396.

Jerauld, G., & Rathmell, J. (1997). Wettability and relative permeability of Prudhoe Bay: A case study in mixed-wet reservoirs. *SPE Reservoir Engineering*, *12*(01), 58-65.

Jo, H., Ahn, H. S., Kang, S., & Kim, M. H. (2011). A study of nucleate boiling heat transfer on hydrophilic, hydrophobic and heterogeneous wetting surfaces. *International Journal of Heat and Mass Transfer, 54*(25), 5643-5652.

Jones, B. J., McHale, J. P., & Garimella, S. V. (2009). The influence of surface roughness on nucleate pool boiling heat transfer. *Journal of Heat Transfer, 131*(12), 121009.

Jones, S., Evans, G., & Galvin, K. (1999). Bubble nucleation from gas cavities—a review. *Advances in colloid and interface science, 80*(1), 27-50.

Jung, Y. C., & Bhushan, B. (2006). Contact angle, adhesion and friction properties of micro-and nanopatterned polymers for superhydrophobicity. *Nanotechnology, 17*(19), 4970.

Kalikmanov, V., Betting, M., Bruining, J., & Smeulders, D. M. (2007). *New developments in nucleation theory and their impact on natural gas separation.* Paper presented at the SPE Annual Technical Conference and Exhibition.

Kandlikar, S. G., Schmitt, D., Carrano, A. L., & Taylor, J. B. (2005). Characterization of surface roughness effects on pressure drop in single-phase flow in minichannels. *Physics of Fluids (1994-present), 17*(10), 100606.

Karimi, A., Fakhroueian, Z., Bahramian, A., Pour Khiabani, N., Darabad, J. B., Azin, R., & Arya, S. (2012). Wettability alteration in carbonates using zirconium oxide nanofluids: EOR implications. *Energy & Fuels, 26*(2), 1028-1036.

Kewen, L., & Abbas, F. (2000). Experimental study of wettability alteration to preferential gas-wetting in porous media and its effects. *SPE Reservoir Evaluation & Engineering, 3*(02), 139-149.

Kumar, V., & Weller, J. (1994). Production of microcellular polycarbonate using carbon dioxide for bubble nucleation. *Journal of engineering for industry, 116*(4), 413-420.

Kurihara, H., & Myers, J. (1960). The effects of superheat and surface roughness on boiling coefficients. *AIChE Journal, 6*(1), 83-91.

Lafuma, A., & Quéré, D. (2003). Superhydrophobic states. *Nature materials, 2*(7), 457-460.

Le Gac, S., Zwaan, E., van den Berg, A., & Ohl, C.-D. (2007). Sonoporation of suspension cells with a single cavitation bubble in a microfluidic confinement. *Lab on a Chip, 7*(12), 1666-1672.

Leung, S. N. S. (2009). *Mechanisms of cell nucleation, growth, and coarsening in plastic foaming: theory, simulation, and experiment.* University of Toronto.

Liger-Belair, G., Parmentier, M., & Jeandet, P. (2006). Modeling the kinetics of bubble nucleation in champagne and carbonated beverages. *The Journal of Physical Chemistry B, 110*(42), 21145-21151.

Lillico, D., Babchin, A., Jossy, W., Sawatzky, R., & Yuan, J.-Y. (2001). Gas bubble nucleation kinetics in a live heavy oil. *Colloids and Surfaces A: Physicochemical and Engineering Aspects, 192*(1), 25-38.

Lubetkin, S. (1995). The fundamentals of bubble evolution. *Chemical Society Reviews, 24*(4), 243-250.

Lubetkin, S., & Blackwell, M. (1988). The nucleation of bubbles in supersaturated solutions. *Journal of colloid and interface science, 126*(2), 610-615.

Maris, H. J. (2006). Introduction to the physics of nucleation. *Comptes Rendus Physique, 7*(9), 946-958.

Miller, J. D., Veeramasuneni, S., Drelich, J., Yalamanchili, M., & Yamauchi, G. (1996). Effect of roughness as determined by atomic force microscopy on the wetting properties of PTFE thin films. *Polymer Engineering & Science, 36*(14), 1849-1855.

Perelaer, J., Hendriks, C. E., de Laat, A. W., & Schubert, U. S. (2009). One-step inkjet printing of conductive silver tracks on polymer substrates. *Nanotechnology, 20*(16), 165303.

Phan, H. T., Caney, N., Marty, P., Colasson, S., & Gavillet, J. (2009). How does surface wettability influence nucleate boiling? *Comptes Rendus Mecanique, 337*(5), 251-259.

Prabhu, K., Fernandes, P., & Kumar, G. (2009). Effect of surface roughness on wetting characteristics of vegetable oils. *Materials and Design, 30*, 297-305.

Pruppacher, H. R., Klett, J. D., & Wang, P. K. (1998). Microphysics of clouds and precipitation.

Ryan, W. L., & Hemmingsen, E. A. (1993). Bubble formation in water at smooth hydrophobic surfaces. *Journal of colloid and interface science, 157*(2), 312-317.

Ryan, W. L., & Hemmingsen, E. A. (1998). Bubble formation at porous hydrophobic surfaces. *Journal of colloid and interface science, 197*(1), 101-107.

Sakai, M., Yanagisawa, T., Nakajima, A., Kameshima, Y., & Okada, K. (2008). Effect of surface structure on the sustainability of an air layer on superhydrophobic coatings in a water− ethanol mixture. *Langmuir, 25*(1), 13-16.

Sear, R. P. (2007). Nucleation: theory and applications to protein solutions and colloidal suspensions. *Journal of Physics: Condensed Matter, 19*(3), 033101.

Skripov, V. P. (1974). *Metastable liquids*: Wiley.

Son, Y., Kim, C., Yang, D. H., & Ahn, D. J. (2008). Spreading of an inkjet droplet on a solid surface with a controlled contact angle at low Weber and Reynolds numbers. *Langmuir, 24*(6), 2900-2907.

Vargaftik, N., Volkov, B., & Voljak, L. (1983). International tables of the surface tension of water. *Journal of Physical and Chemical Reference Data, 12*(3), 817-820.

Venter, J. C., Adams, M. D., Myers, E. W., Li, P. W., Mural, R. J., Sutton, G. G., . . . Holt, R. A. (2001). The sequence of the human genome. science, 291(5507), 1304-1351.

Wen, D., & Wang, B. (2002). Effects of surface wettability on nucleate pool boiling heat transfer for surfactant solutions. *International Journal of Heat and Mass Transfer, 45*(8), 1739-1747.

Wenzel, R. N. (1936). Resistance of solid surfaces to wetting by water. *Industrial & Engineering Chemistry, 28*(8), 988-994.

Wienecke, M., Luke, A., Gorenflo, D., & Span, R. (2005). Flow boiling of highly viscous fluids in a vertical annular tube. *Chemical Engineering Research and Design, 83*(8), 1044-1051.

Wilt, P. (1986). Nucleation rates and bubble stability in water-carbon dioxide solutions. *Journal of colloid and interface science, 112*(2), 530-538.

Yang, C. T., Smith, T. G., Bigio, D. I., & Anolick, C. (1997). Polymer trace devolatilization: I. Foaming experiments and model development. *AIChE Journal, 43*(7), 1861-1873.

Yang, H., & Jiang, P. (2010). Self-cleaning diffractive macroporous films by doctor blade coating. *Langmuir, 26*(15), 12598-12604.

Yuan, H., Tan, S., Feng, L., & Liu, X. (2016). Heterogeneous bubble nucleation on heated surface from insoluble gas. *International Journal of Heat and Mass Transfer, 101*, 1185-1192.

Zhao, X., Blunt, M. J., & Yao, J. (2010). Pore-scale modeling: Effects of wettability on waterflood oil recovery. *Journal of Petroleum Science and Engineering, 71*(3), 169-178.

VITA

RUAA JASIM QADER

Candidate for the Degree of

Master of Science

Thesis: INFLUENCE OF WETTABILITY ON GAS BUBBLE NUCLEATION

Major Field: Chemical Engineering

Biographical: Ruaa is Iraqi citizen was born and raised in Baghdad. Ruaa earned her bachelor degree from the University of Baghdad. She has worked for the Ministry of Natural Resources in Erbil/Iraq as a petroleum engineer, later; she got training in oil fields as a drilling engineer. Before she got the scholarship from Kurdistan Regional Government to continue her master degree in the United States, she worked in MI- Swaco Schlumberger Lab Company in Erbil for one and a half year. Ruaa is planning to work in the industry field for several years for the sake of gaining the required experience to be a professional chemical/petroleum engineer prior establishing her own company.

Education:

Completed the requirements for the Master of Science in Chemical Engineering at Oklahoma State University, Stillwater, Oklahoma in July 2016.

Completed the requirements for the Bachelor of Science in Petroleum Engineering at University of Bagdad/College of Engineering, Baghdad, Iraq/2006.